(ketoprofen) for the genetic rHSA dimer were also determined by ultrafiltration using ^{3}H-labeled CMPF and ^{14}C-labeled ketoprofen, respectively. The results were the same as those for the BMH-bridged rHSA dimer, the binding constants (k) of both CMPF and ketoprofen for the genetic rHSA dimer were similar to those for the HSA monomer. These results suggest that the binding site and binding capacity of the HSA monomer were preserved in the HSA dimer.

Disposition

Komatsu et al.[47] injected the rHSA monomer or BMH-bridged rHSA dimer labeled with ^{125}I (^{125}I–rHSA monomer or ^{125}I–rHSA dimer) into rats at a dose of 1.0 mg/kg, and evaluated the time course for both ^{125}I-labeled proteins in the blood circulation. The retention of the rHSA dimer in the blood was increased compared with that for the rHSA monomer, and the $t_{1/2}$ values calculated from the plasma concentration curve were 8.9 and 16.2 h for the monomer and dimer, respectively. In addition, the BMH-bridged rHSA dimer was distributed in the skin, liver, kidney, and spleen, similar to the rHSA monomer.[47] The pharmacokinetics of the ^{125}I-labeled native HSA and genetic rHSA dimer were evaluated in rats at a dose of 0.1 mg/kg. The $t_{1/2}$ for the ^{125}I–genetic rHSA dimer was increased by about 1.5 times as compared with those of ^{125}I-native HSA. These results suggest that the ^{125}I–rHSA dimer has a better retention in the blood circulation as compared with ^{125}I–native HSA.[29]

On the contrary, McCurdy et al.[46] reported that a recombinant rabbit serum albumin (rRSA) dimer was cleared more rapidly ($t_{1/2}$: 3.0 days) in rabbits than the corresponding C34A rRSA monomer ($t_{1/2}$: 4.9 days). The dimer in this case was a C34A rRSA mutant modified by the addition of an N-terminal hexahistidinyl tag, which was joined via a hexaglycine spacer through the C terminus to the N terminus of another His-tagged C34A rRSA.[46] These contradictory results may be attributable to species differences, as shown by Sheffield et al.[59] or to structural differences caused by the His tag.

In addition to the study on disposition under normal conditions, the dispositions of BMH-bridged and genetic rHSA dimer in several pathological conditions have also been examined. Matsushita et al.[29] evaluated the vascular permeability of the ^{125}I–genetic rHSA dimer (0.1 mg/kg) using a carrageenan-induced paw edema mouse model. The low vascular permeability of the ^{125}I–rHSA dimer was observed compared with that of ^{125}I–native HSA. These results suggest that the escape of HSA to the extravascular space during inflammation can be reduced by dimerization. Furthermore, they also evaluated the pharmacokinetics of ^{125}I-labeled native HSA and the genetic rHSA dimer in carrageenan-air-pouch rats. A significant difference in $t_{1/2}$ was observed, and this model also showed an improvement in the retention of ^{125}I–rHSA dimer in the blood. These results clearly showed a longer blood retention and lower vascular permeability of the rHSA dimer in comparison with native HSA.

The pharmacokinetic properties of the BMH-bridged rHSA dimer were evaluated in nephrotic rats (1 mg/kg) induced by treatment with doxorubicin, which has a high glomerular permeability.[60] The plasma rHSA monomer was rapidly cleared compared with the BMH-bridged rHSA dimer in nephrotic rats, and interestingly the plasma concentration of the BMH-bridged rHSA dimer in nephrotic rats was similar to that in normal rats. Furthermore, the accumulation of the BMH-bridged rHSA dimer in the kidney was dramatically decreased compared with that for the rHSA monomer, and the urinary excretion of the BMH-bridged rHSA dimer was decreased by half compared with that after the administration of the rHSA monomer. In addition, the renal clearance of the rHSA monomer was 1.81 ± 0.46 mL/h, whereas that of BMH-bridged rHSA dimer was 0.20 ± 0.12 mL/h in nephrotic rats. These findings suggest that the HSA dimer has high blood retention properties in normal conditions as well as under conditions of high permeability.

Ishima et al.[61] carried out pharmacokinetic studies of rHSA monomers and genetic rHSA dimers in a C26 solid tumor model. They intravenously administered both protein solutions via the tail vein at a dose of 1 mg/kg and evaluated the plasma retention and tumor accumulation of the rHSA monomer and dimer 24 h after the injection. At 24 h after the injection, the level of accumulation of the genetic rHSA dimer in the tumor tissue was 1.8 times higher than that for the rHSA monomer. In addition, the genetic rHSA dimer showed a much higher level of blood retention compared with that of the rHSA monomer. One of the developing strategies for enhancing the tumor-specific delivery of the therapeutics is albumin-based drug delivery technology, which can enhance drug targeting and improve the pharmacokinetic profile of various therapeutic drugs.[30,62,63] It thus appears that the genetic rHSA dimer would be a good candidate as a drug carrier because in addition to a prolonged blood retention it accumulates well in tumor tissue.

POTENTIAL MEDICAL APPLICATIONS

The albumin dimer has potential for use as a drug carrier and novel plasma expander because of its physicochemical properties, especially colloid osmotic pressure, and pharmacokinetic properties. Some studies have reported the possibility of using the albumin

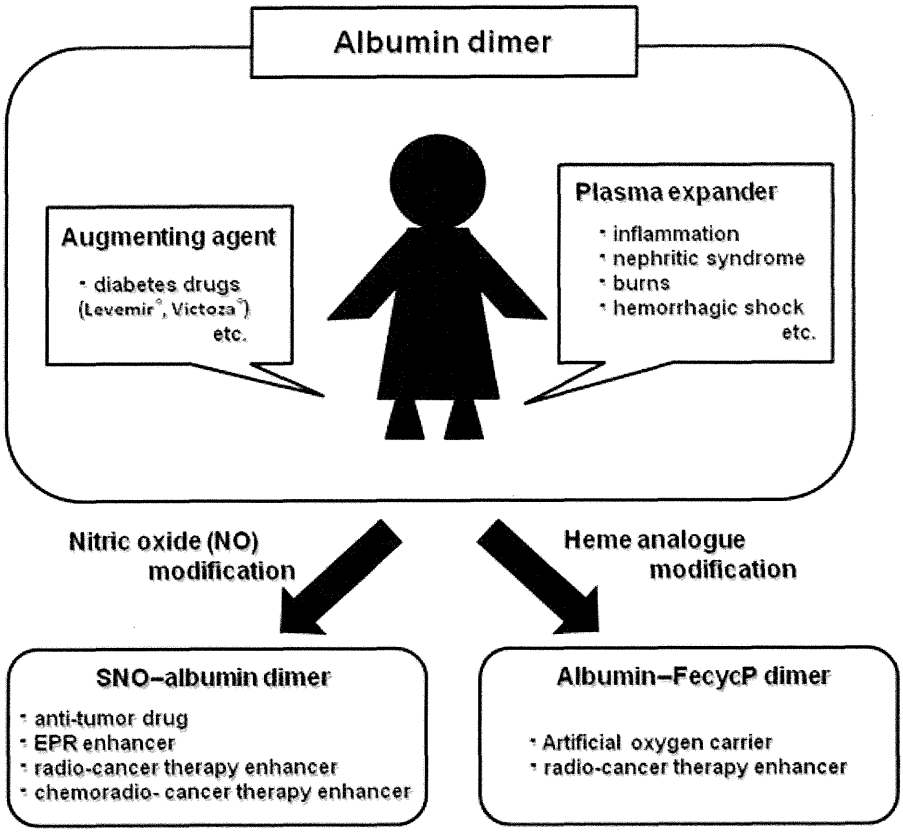

Figure 5. Summary of albumin dimer and its modifications for pharmaceutical applications.

dimer for medical applications, which are given below (Fig. 5).

Plasma Expander

HSA is used as a plasma expander and is particularly useful when it is given in the form of an infusion to patients with hypoalbuminemia. For many years, it was generally thought that albumin infusions improved life expectancy.[64,65] Nevertheless, a *meta*-analysis report concluded that albumin infusions can be potentially harmful to critically ill patients, and evidence in support of the administration of albumin infusion in reducing mortality in critically ill patients with hypoalbuminemia is lacking.[66] As it is well known that capillary permeability is increased in many pathological and physiological conditions and that this increased response is accompanied by an increased plasma proteins including HSA flux to the extravascular compartment, infused HSA fails to function as a plasma expander in such clinical conditions. Instead, ironically the administered HSA is transported to organs or extravasated, causing edema and, hence, worsening the disease. In view of this therapeutic problem of albumin infusion, a new type of HSA preparation that can maintain albumin concentration even under conditions of increased capillary permeability would be highly desirable. To overcome this issue, increasing the molecular size of HSA by genetic or chemical dimerization may be the best strategy.[67]

As described in the "*Disposition*" section, Matsushita et al.[29] demonstrated the effect of an increase in vascular permeability during inflammation on a genetic rHSA dimer using carrageenan-induced paw edema in mice, which exhibit a biphasic inflammation response,[68] and carrageenan-air-pouch rats, which were used to evaluate acute exudative stage and the chronic proliferative stage of carrageenan-air-pouch inflammation.[69] In this model, the movement of the native HSA monomer to the extravascular space during inflammation can be reduced by dimerization. Furthermore, the utility of the BMH-bridged rHSA dimer under nephrotic conditions, which is severe protein permeability condition, was evaluated to verify the potential of the rHSA dimer for use as a versatile plasma expander.[60] This model also showed an improvement in the retention of BMH-bridged rHSA dimer in the blood due to a reduction in renal distribution and urinary excretion. The glomerular biological membrane has properties that allow for high filtration rates of water and small- and mid-sized molecules but does not allow larger proteins such as HSA to be filtered. These restrictions can be explained by several mechanisms, including charge repulsion in the glomerular basement membrane and a

barrier, depending on their molecular sizes.[70] However, in the cases of the nephritic syndrome, infused HSA monomer is easily filtered by the renal glomerulus because of the destruction of the glomerulus. In contrast, the rHSA dimer showed better blood retention properties, even under severe high permeability conditions, due to its larger molecular mass (~130 kDa), than HSA monomer and retention of negative charge as the HSA monomer (isoelectric point, $pI = 4.8$).

These findings support the conclusion that the rHSA dimer has the potential for use as a new plasma volume expander because it showed superior blood retention characteristics in various clinical situations. Furthermore, its use would allow reduction of multiple administrations required as in the case of conventional HSA preparations and could be quite cost-effective.

Augmenting Agent for Diabetes Drugs

Patients with diabetes frequently suffer from diabetes-related complications such as diabetic nephropathy. As diabetic nephropathy progresses to end-stage renal failure, hypoalbuminemia is usually induced. Liraglutide (Victoza®, Novo Nordisk, Princeton, NJ) is a new type of diabetes drug, and is an albumin-binding derivative of the glucagon-like 1 peptide (GLP-1) in which this peptide hormone is derivatized with myristic acid at the ε-amino position of lysine introduced at the N-terminal position of glutamic acid in the GLP-1 peptide sequence.[71,72] Native GLP-1 has a $t_{1/2}$ of 1.5–2 min due to degradation by ubiquitous enzymes. In contrast to GLP-1, liraglutide is stable against metabolic degradation due to the fact that it is bound to albumin and has a plasma $t_{1/2}$ of 11–15 h after subcutaneous administration.[73] This indicates that liraglutide cannot completely provide a pharmacological benefit, when the albumin concentration in blood is declining. In addition, Levemir® (Novo Nordisk, Bagsvaerd, Denmark), an albumin-binding derivative of human insulin, is also approved for the treatment of types 1 and 2 diabetes. It is engineered by omitting the C-terminal amino acid threonine from recombinant human insulin and attaching a myristic acid residue to the introduced amino acid lysine. Levemir® binds to HSA in the blood circulation because of its high affinity for HSA ($K_d = \sim 0.05$ μM), the $t_{1/2}$ of Levemir® is extended from 4–6 min for native human insulin to 5–7 hours for Levemir®.[10]

A pharmacokinetic study of the BMH-bridged rHSA dimer showed that the $t_{1/2}$ for the BMH-bridged rHSA dimer was 1.5 times longer than that of the rHSA monomer in streptozotocin-induced diabetic rats (preparation for submission). In addition, the binding site and binding capacity in the BMH-bridged rHSA dimer were preserved, that is, the same as those in HSA monomer, and native HSA has at least five binding sites for myristic acid. These findings indicate that the BMH-bridged rHSA dimer sustains the ability for the binding of liraglutide. Therefore, the HSA dimer would also function as an augmenting agent for diabetes drugs, in particular, the albumin-binding derivative of GLP-1 (Victoza®) and insulin (Levemir®).

Antitumor Drugs with Augmented EPR Effect

Nitric oxide (NO) has been shown to have potential for use in cancer therapy and it is emerging as an antioncogenic agent in contrast to conventional therapeutic agents.[74,75] Therefore, many attempts have been made to develop new antitumor drugs using a number of NO donors, such as *S*-nitrosoglutathione, but these have not proceeded to clinical application because of problems such as toxicity at high concentrations due to a lack of specificity for tumor cells or side effects that can occur during long-term applications.[76–78] On the contrary, albumin has received broad attention as a suitable protein for transporting NO because NO binds to Cys34 of albumin to form *S*-nitrosylated HSA.[79,80] Therefore, HSA is a good candidate not only for an efficient carrier of NO but also as an antitumor drug because of its ability to promote the uptake of drugs in tumor tissue via EPR effects.[81,82] The HSA dimer is also expected to have an enhanced accumulation in solid tumors via the EPR mechanism[83,84] because of its high molecular weight (~130 kDa).

Ishima et al.[61] developed a *S*-nitrosated genetic rHSA dimer (SNO-dimer), and examined its potential for anticancer therapeutics. They performed a biodistribution analysis of the SNO dimer given to C26-tumor-bearing mice, and found that the accumulation of SNO dimer in the tumor tissue was 2.6 times higher than that of the SNO monomer at 24 h after injection. In addition, cell death, as evidenced by the quantification of the release of extracellular lactate dehydrogenase (LDH), clearly showed that treatment with the SNO dimer resulted in a much more pronounced LDH release from the cells and that this release was NO dose dependent. Thus, the SNO dimer appears to be a good candidate as an antitumor drug because in addition to a good accumulation in tumor tissue it has cancer cell death activity.

Furthermore, they focused on the difference between the accumulation of genetic rHSA dimer and SNO dimer in tumor tissue. The accumulation of the SNO dimer in tumor tissue was 1.6 times higher than that of the genetic rHSA dimer. This suggests that *S*-nitrosation of the dimer further enhanced its EPR effect, probably via the release of NO from the SNO dimer, similar to the effect of nitroglycerin.[85] To evaluate whether SNO dimer enhances the EPR effect by delivering NO, they determined the extravasation of Evans blue in the tumor tissue after treatment with

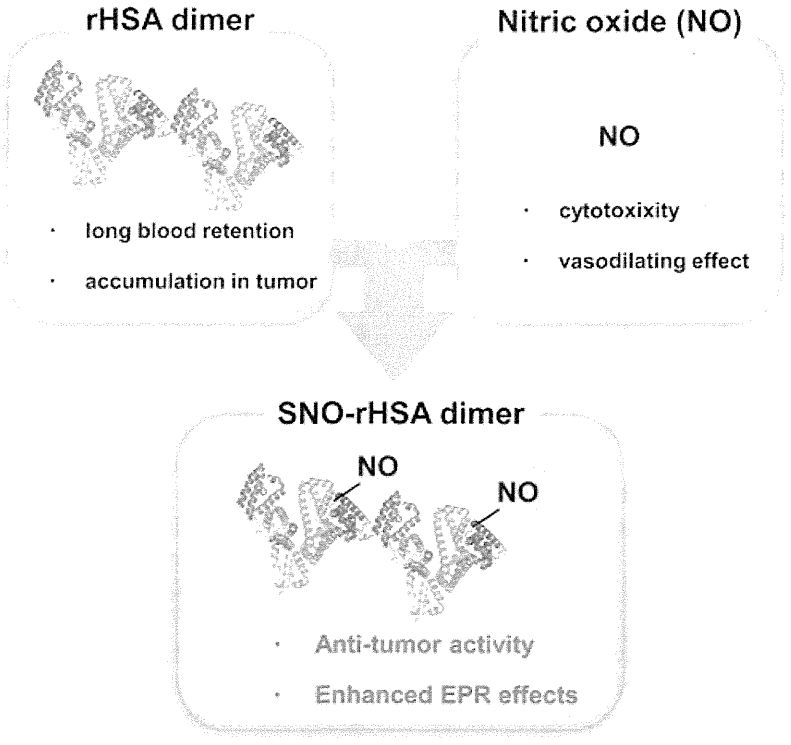

Figure 6. Formation and potential medical therapy for tumors using the SNO dimer.

the SNO dimer compared with the SNO monomer, using C26-tumor-bearing mice as an *in vivo* model. As a result, the extravasation of Evans blue dye in tumor tissue by intravenous treatment with the SNO dimer, but not in muscle, was increased by more than twice and three times, respectively, compared with the SNO monomer and control, indicating that the SNO dimer enhanced the EPR effect.

On the basis of these findings, SNO dimer possesses the dual effects for anticancer therapy. The SNO dimer has clinical possibilities for being not only an anticancer drug but also a valuable tumor-targeting delivery system due to enhancement of the EPR effect (Fig. 6). Furthermore, it was reported that an NO donor could attenuate hypoxia-induced chemoresistance and enhanced radiosensitivity via the reduction of hypoxic condition.[86–89] These findings suggested that combinational use of the SNO dimer with conventional radiotherapy or chemoradiotherapy may be a novel therapeutic strategy for cancer treatment.

Artificial Oxygen Carriers

Several types of artificial oxygen carriers have been developed and some are currently at the stage of clinical development.[90–93] However, among them, only polymerized bovine-derived hemoglobin (Hemopure; Biopure Corporation, Cambridge, Massachusetts) has been approved for limited use in South Africa.[94] Tsuchida et al.[95] synthesized an HSA-based artificial oxygen carrier "albumin-heme," which carries a maximum of eight molecules of synthetic heme with a covalently bound proximal base incorporated into the hydrophobic cavities of rHSA. It can reversibly bind and release oxygen under physiological conditions similar to hemoglobin.[96,97] This oxygen-carrying plasma protein has been proven to act as a RBC substitute *in vitro* and *in vivo*.[98,99] In addition, an *in vivo* study using hemorrhagic shocked rats also revealed that the renal cortical oxygen tensions and skeletal tissue oxygen tensions were increased when albumin–heme was injected.[100,101] However, the albumin–heme solution with a physiological HSA concentration involves 6 mM of heme, which corresponds to only 65% of the amount in human blood. Therefore, a highly condensed solution could solve this problem, but colloid osmotic pressure increases in proportion to the albumin concentration. In addition, an artificial oxygen carrier is also required to maintain a high blood circulation because it must temporarily function until a blood transfusion is available or until autologous blood is recovered after a massive hemorrhage.

To overcome these problems, Komatsu et al.[47] synthesized the 2-[8-{N-(2-methylimidazolyl)}-octanoyloxymethyl]-5,10,15,20-tetrakis{α,α,α,α-o-(1-methylcyclohexanamido)phenyl}porphinatoiron(II) (FecycP), and incorporated it into the BMH-bridged rHSA dimer. One molecule of the BMH-bridged rHSA dimer incorporates 16 FecycPs, which is exactly twice the amount compared with that of the monomeric rHSA, and the resulting hemoprotein can reversibly

bind and release oxygen under physiological conditions. The rHSA–FecycP dimer solution (8.5 g/dL) satisfies the initial clinical requirements for an oxygen carrier as an RBC substitute, which transports 10 mM oxygen (compared with 9.2 mM in the human blood) while maintaining the colloid osmotic pressure at a constant pressure of 19 Torr. Furthermore, the rHSA dimer is retained in the blood for longer periods of time than the HSA monomer. Therefore, the rHSA–FecycP dimer promises to be a new type of oxygen carrier that has not only oxygen carrying capacity, but also is efficiently retained in the circulating blood. Furthermore, tumor-cell hypoxia is one of the main factors inducing radioresistance. It was reported that albumin–heme enhances tumor oxygenation and subsequently enhances the response to radiation in an experimental tumor model.[102,103] Because the albumin dimer accumulated in tumors at higher levels than the monomer, the rHSA–FecycP dimer is also a candidate as a radiation-enhancing drug.

CONCLUSION

Since mid-20th century, the presence of Cys34–Cys34 disulfide linked albumin dimer in the blood has been confirmed. However, the dimer was not given much attention for use in clinical application because of several intrinsic problems of the dimer protein molecule. Recently, a number of attempts have been made to overcome the problems of Cys34–Cys34 disulfide-linked albumin dimer. These include binding two HSA with a flexible spacer such as BMH chemically and amino acid linker genetically. A substantial body of scientific experimental evidences clearly showed that rHSA dimer with a flexible spacer has favorable structural, physicochemical, and pharmacokinetic characteristics for application as plasma expander and drug carrier. Hence, rHSA dimer with a flexible spacer is a new biomaterial with promising potential pharmaceutical and medical uses. Further developmental studies on rHSA dimer are expected to expand its possibility for various clinical applications.

REFERENCES

1. Curry S, Mandelkow H, Brick P, Franks N. 1998. Crystal structure of human serum albumin complexed with fatty acid reveals an asymmetric distribution of binding sites. Nat Struct Biol 5(9):827–835.
2. Otagiri M, Ed. 2011. Human serum albumin: New insight on its structural dynamics, functional impacts and pharmaceutical applications. Kumamoto, Japan: Sojo University Publishing Centre, pp 1–29.
3. Otagiri M, Chuang VT. 2009. Pharmaceutically important pre- and posttranslational modifications on human serum albumin. Biol Pharm Bull 32(4):527–534.
4. Stewart AJ, Blindauer CA, Berezenko S, Sleep D, Tooth D, Sadler PJ. 2005. Role of Tyr84 in controlling the reactivity of Cys34 of human albumin. FEBS J 272(2):353–362.
5. Quinlan GJ, Margarson MP, Mumby S, Evans TW, Gutteridge JM. 1998. Administration of albumin to patients with sepsis syndrome: A possible beneficial role in plasma thiol repletion. Clin Sci (Lond) 95(4):459–465.
6. Quinlan GJ, Mumby S, Martin GS, Bernard GR, Gutteridge JM, Evans TW. 2004. Albumin influences total plasma antioxidant capacity favorably in patients with acute lung injury. Crit Care Med 32(3):755–759.
7. Schnitzer JE. 1992. gp60 is an albumin-binding glycoprotein expressed by continuous endothelium involved in albumin transcytosis. Am J Physiol 262(1 Pt 2):H246–254.
8. Tiruppathi C, Song W, Bergenfeldt M, Sass P, Malik AB. 1997. Gp60 activation mediates albumin transcytosis in endothelial cells by tyrosine kinase-dependent pathway. J Biol Chem 272(41):25968–25975.
9. Wang Z, Tiruppathi C, Minshall RD, Malik AB. 2009. Size and dynamics of caveolae studied using nanoparticles in living endothelial cells. ACS Nano 3(12):4110–4116.
10. Morales J. 2007. Defining the role of insulin detemir in basal insulin therapy. Drugs 67(17):2557–2584.
11. Flisiak R, Flisiak I. 2010. Albinterferon-alpha 2b: A new treatment option for hepatitis C. Expert Opin Biol Ther 10(10):1509–1515.
12. Goyen M. 2008. Gadofosveset-enhanced magnetic resonance angiography. Vasc Health Risk Manag 4(1):1–9.
13. Wittebole X, Hantson P. 2011. Use of the molecular adsorbent recirculating system (MARS) for the management of acute poisoning with or without liver failure. Clin Toxicol (Phila) 49(9):782–793.
14. Adams BK, Al Attia HM, Khadim RA, Al Haider ZY. 2001. 99Tc(m) nanocolloid scintigraphy: A reliable way to detect active joint disease in patients with peripheral joint pain. Nucl Med Commun 22(3):315–318.
15. Kim HK, Kim S, Park JJ, Jeong JM, Mok YJ, Choi YH. 2011. Sentinel node identification using technetium–99m neomannosyl human serum albumin in esophageal cancer. Ann Thorac Surg 91(5):1517–1522.
16. Rink T, Heuser T, Fitz H, Schroth HJ, Weller E, Zippel HH. 2001. Lymphoscintigraphic sentinel node imaging and gamma probe detection in breast cancer with Tc–99m nanocolloidal albumin: results of an optimized protocol. Clin Nucl Med 26(4):293–298.
17. Ding R, Frei E, Fardanesh M, Schrenk HH, Kremer P, Haefeli WE. 2011. Pharmacokinetics of 5-aminofluorescein-albumin, a novel fluorescence marker of brain tumors during surgery. J Clin Pharmacol 51(5):672–678.
18. Giannoukakis N. 2003. CJC-1131. ConjuChem. Curr Opin Investig Drugs 4(10):1245–1249.
19. Unger C, Haring B, Medinger M, Drevs J, Steinbild S, Kratz F, Mross K. 2007. Phase I and pharmacokinetic study of the (6-maleimidocaproyl)hydrazone derivative of doxorubicin. Clin Cancer Res 13(16):4858–4866.
20. Nelson DR, Benhamou Y, Chuang WL, Lawitz EJ, Rodriguez-Torres M, Flisiak R, Rasenack JW, Kryczka W, Lee CM, Bain VG, Pianko S, Patel K, Cronin PW, Pulkstenis E, Subramanian GM, McHutchison JG. 2010. Albinterferon alfa-2b was not inferior to pegylated interferon-alpha in a randomized trial of patients with chronic hepatitis C virus genotype 2 or 3. Gastroenterology 139(4):1267–1276.
21. Zeuzem S, Sulkowski MS, Lawitz EJ, Rustgi VK, Rodriguez-Torres M, Bacon BR, Grigorescu M, Tice AD, Lurie Y, Cianciara J, Muir AJ, Cronin PW, Pulkstenis E, Subramanian GM, McHutchison JG. 2010. Albinterferon alfa-2b was not inferior to pegylated interferon-alpha in a randomized trial of patients with chronic hepatitis C virus genotype 1. Gastroenterology 139(4):1257–1266.
22. Furukawa M, Tanaka R, Chuang VT, Ishima Y, Taguchi K, Watanabe H, Maruyama T, Otagiri M. 2011. Human serum

albumin–thioredoxin fusion protein with long blood retention property is effective in suppressing lung injury. J Control Release 154(2):189–195.
23. Wang W, Ou Y, Shi Y. 2004. AlbuBNP, a recombinant B-type natriuretic peptide and human serum albumin fusion hormone, as a long-term therapy of congestive heart failure. Pharm Res 21(11):2105–2111.
24. Bae S, Ma K, Kim TH, Lee ES, Oh KT, Park ES, Lee KC, Youn YS. 2012. Doxorubicin-loaded human serum albumin nanoparticles surface-modified with TNF-related apoptosis-inducing ligand and transferrin for targeting multiple tumor types. Biomaterials 33(5):1536–1546.
25. Ozgur A, Lambrecht FY, Ocakoglu K, Gunduz C, Yucebas M. 2012. Synthesis and biological evaluation of radiolabeled photosensitizer linked bovine serum albumin nanoparticles as a tumor imaging agent. Int J Pharm 422(1–2):472–478.
26. Cabrales P, Tsai AG, Ananda K, Acharya SA, Intaglietta M. 2008. Volume resuscitation from hemorrhagic shock with albumin and hexaPEGylated human serum albumin. Resuscitation 79(1):139–146.
27. Martini J, Cabrales P, KA, Acharya SA, Intaglietta M, Tsai AG. 2008. Survival time in severe hemorrhagic shock after perioperative hemodilution is longer with PEG-conjugated human serum albumin than with HES 130/0.4: A microvascular perspective. Crit Care 12(2):R54.
28. Komatsu T, Hamamatsu K, Tsuchida E. 1999. Cross-linked human serum albumin dimer incorporating sixteen (tetraphenylporphinato)iron(II) derivatives: Synthesis, characterization, and O_2-binding property. Macromolecules 32:8388–8391.
29. Matsushita S, Chuang VT, Kanazawa M, Tanase S, Kawai K, Maruyama T, Suenaga A, Otagiri M. 2006. Recombinant human serum albumin dimer has high blood circulation activity and low vascular permeability in comparison with native human serum albumin. Pharm Res 23(5):882–891.
30. Dennis MS, Zhang M, Meng YG, Kadkhodayan M, Kirchhofer D, Combs D, Damico LA. 2002. Albumin binding as a general strategy for improving the pharmacokinetics of proteins. J Biol Chem 277(38):35035–35043.
31. Hirata K, Maruyama T, Watanabe H, Maeda H, Nakajou K, Iwao Y, Ishima Y, Katsumi H, Hashida M, Otagiri M. 2010. Genetically engineered mannosylated-human serum albumin as a versatile carrier for liver-selective therapeutics. J Control Release 145(1):9–16.
32. Lu W, Wan J, She Z, Jiang X. 2007. Brain delivery property and accelerated blood clearance of cationic albumin conjugated pegylated nanoparticle. J Control Release 118(1):38–53.
33. Xu F, Lu W, Wu H, Fan L, Gao X, Jiang X. 2009. Brain delivery and systemic effect of cationic albumin conjugated PLGA nanoparticles. J Drug Target 17(6):423–434.
34. Scorza G, Minetti M. 1998. One-electron oxidation pathway of thiols by peroxynitrite in biological fluids: Bicarbonate and ascorbate promote the formation of albumin disulphide dimers in human blood plasma. Biochem J 329 (Pt 2):405–413.
35. Ogasawara Y, Namai T, Togawa T, Ishii K. 2006. Formation of albumin dimers induced by exposure to peroxides in human plasma: A possible biomarker for oxidative stress. Biochem Biophys Res Commun 340(2):353–358.
36. Mimic-Oka J, Simic T, Djukanovic L, Reljic Z, Davicevic Z. 1999. Alteration in plasma antioxidant capacity in various degrees of chronic renal failure. Clin Nephrol 51(4):233–241.
37. Richard MJ, Arnaud J, Jurkovitz C, Hachache T, Meftahi H, Laporte F, Foret M, Favier A, Cordonnier D. 1991. Trace elements and lipid peroxidation abnormalities in patients with chronic renal failure. Nephron 57(1):10–15.
38. Edsall JT, Maybury RH, Simpson RB, Straessle R. 1954. Dimerization of serum mercaptalbumin in presence of mercurials. II. Studies with a bifunctional organic mercurial. J Am Chem Soc 76:3131–3138.
39. Straessle R. 1954. A disulfide dimer of human mercaptalbumin1a,b. J Am Chem Soc 76:3138–3142.
40. Andersson LO. 1970. Hydrolysis of disulfide bonds in weakly alkaline media. II. Bovine serum albumin dimer. Biochim Biophys Acta 200(2):363–369.
41. Sollenne NP, Wu HL, Means GE. 1981. Disruption of the tryptophan binding site in the human serum albumin dimer. Arch Biochem Biophys 207(2):264–269.
42. Carter DC, Ho JX. 1994. Structure of serum albumin. Adv Protein Chem 45:153–203.
43. Cornell CN, Chang R, Kaplan LJ. 1981. The environment of the sulfhydryl group in human plasma albumin as determined by spin labeling. Arch Biochem Biophys 209(1):1–6.
44. Curry S, Brick P, Franks NP. 1999. Fatty acid binding to human serum albumin: New insights from crystallographic studies. Biochim Biophys Acta 1441(2–3):131–140.
45. Sugio S, Kashima A, Mochizuki S, Noda M, Kobayashi K. 1999. Crystal structure of human serum albumin at 2.5 Å resolution. Protein Eng 12(6):439–446.
46. McCurdy TR, Gataiance S, Eltringham-Smith LJ, Sheffield WP. 2004. A covalently linked recombinant albumin dimer is more rapidly cleared in vivo than are wild-type and mutant C34A albumin. J Lab Clin Med 143(2):115–124.
47. Komatsu T, Oguro Y, Teramura Y, Takeoka S, Okai J, Anraku M, Otagiri M, Tsuchida E. 2004. Physicochemical characterization of cross-linked human serum albumin dimer and its synthetic heme hybrid as an oxygen carrier. Biochim Biophys Acta 1675(1–3):21–31.
48. Gustavsson M, Lehtio J, Denman S, Teeri TT, Hult K, Martinelle M. 2001. Stable linker peptides for a cellulose-binding domain–lipase fusion protein expressed in *Pichia pastoris*. Protein Eng 14(9):711–715.
49. Shan D, Press OW, Tsu TT, Hayden MS, Ledbetter JA. 1999. Characterization of scFv–Ig constructs generated from the anti-CD20 mAb 1F5 using linker peptides of varying lengths. J Immunol 162(11):6589–6595.
50. Takemura S, Asano R, Tsumoto K, Ebara S, Sakurai N, Katayose Y, Kodama H, Yoshida H, Suzuki M, Imai K, Matsuno S, Kudo T, Kumagai I. 2000. Construction of a diabody (small recombinant bispecific antibody) using a refolding system. Protein Eng 13(8):583–588.
51. Watanabe H, Yamasaki K, Kragh-Hansen U, Tanase S, Harada K, Suenaga A, Otagiri M. 2001. In vitro and in vivo properties of recombinant human serum albumin from *Pichia pastoris* purified by a method of short processing time. Pharm Res 18(12):1775–1781.
52. Peter JT, Ed. 1996. All about albumin, genetics, and medical application. San Diego: Academic Press, pp 432.
53. Beilby JP, Chin C, Garcia-Webb P, Bhagat CI. 1985. An albumin dimer in urine. Clin Chem 31(3):478–479.
54. Birtwistle RJ, Hardwicke J. 1985. The role of urea in albumin dimerisation in nephrotic urines. Clin Chim Acta 151(1):41–48.
55. Sudlow G, Birkett DJ, Wade DN. 1975. The characterization of two specific drug binding sites on human serum albumin. Mol Pharmacol 11(6):824–832.
56. Sudlow G, Birkett DJ, Wade DN. 1976. Further characterization of specific drug binding sites on human serum albumin. Mol Pharmacol 12(6):1052–1061.
57. Bloomfield V. 1966. The structure of bovine serum albumin at low pH. Biochemistry 5(2):684–689.
58. Squire PG, Moser P, O'Konski CT. 1968. The hydrodynamic properties of bovine serum albumin monomer and dimer. Biochemistry 7(12):4261–4272.

59. Sheffield WP, Mamdani A, Hortelano G, Gataiance S, Eltringham-Smith L, Begbie ME, Leyva RA, Liaw PS, Ofosu FA. 2004. Effects of genetic fusion of factor IX to albumin on in vivo clearance in mice and rabbits. Br J Haematol 126(4):565–573.
60. Taguchi K, Urata Y, Anraku M, Watanabe H, Kawai K, Komatsu T, Tsuchida E, Maruyama T, Otagiri M. 2010. Superior plasma retention of a cross-linked human serum albumin dimer in nephrotic rats as a new type of plasma expander. Drug Metab Dispos 38(12):2124–2129.
61. Ishima Y, Chen D, Fang J, Maeda H, Minomo A, Kragh-Hansen U, Maruyama T, Otagiri M. 2012. S-Nitrosated human serum albumin dimer is not only a novel anti-tumor drug but also a potentiator for anti-tumor drugs with augmented EPR effects. Bioconjug Chem 23(2):264–271.
62. Burger AM, Hartung G, Stehle G, Sinn H, Fiebig HH. 2001. Pre-clinical evaluation of a methotrexate–albumin conjugate (MTX–HSA) in human tumor xenografts in vivo. Int J Cancer 92(5):718–724.
63. Wosikowski K, Biedermann E, Rattel B, Breiter N, Jank P, Loser R, Jansen G, Peters GJ. 2003. In vitro and in vivo antitumor activity of methotrexate conjugated to human serum albumin in human cancer cells. Clin Cancer Res 9(5):1917–1926.
64. Vincent JL, Navickis RJ, Wilkes MM. 2004. Morbidity in hospitalized patients receiving human albumin: A meta-analysis of randomized, controlled trials. Crit Care Med 32(10):2029–2038.
65. Wilkes MM, Navickis RJ. 2001. Patient survival after human albumin administration. A meta-analysis of randomized, controlled trials. Ann Intern Med 135(3):149–164.
66. Reviewers CIGA. 1998. Human albumin administration in critically ill patients: Systematic review of randomised controlled trials. Cochrane Injuries Group Albumin Reviewers. BMJ 317(7153):235–240.
67. Niemi TT, Miyashita R, Yamakage M. 2010. Colloid solutions: A clinical update. J Anesth 24(6):913–925.
68. Posadas I, Bucci M, Roviezzo F, Rossi A, Parente L, Sautebin L, Cirino G. 2004. Carrageenan-induced mouse paw oedema is biphasic, age-weight dependent and displays differential nitric oxide cyclooxygenase-2 expression. Br J Pharmacol 142(2):331–338.
69. Sato H, Hashimoto M, Sugio K, Ohuchi K, Tsurufuji S. 1980. Comparative study between steroidal and nonsteroidal anti-inflammatory drugs on the mode of their actions on vascular permeability in rat carrageenin-air-pouch inflammation. J Pharmacobiodyn 3(7):345–352.
70. Haraldsson B, Nystrom J, Deen WM. 2008. Properties of the glomerular barrier and mechanisms of proteinuria. Physiol Rev 88(2):451–487.
71. Elsadek B, Kratz F. 2012. Impact of albumin on drug delivery—New applications on the horizon. J Control Release 157(1):4–28.
72. Knudsen LB, Nielsen PF, Huusfeldt PO, Johansen NL, Madsen K, Pedersen FZ, Thogersen H, Wilken M, Agerso H. 2000. Potent derivatives of glucagon-like peptide-1 with pharmacokinetic properties suitable for once daily administration. J Med Chem 43(9):1664–1669.
73. Degn KB, Juhl CB, Sturis J, Jakobsen G, Brock B, Chandramouli V, Rungby J, Landau BR, Schmitz O. 2004. One week's treatment with the long-acting glucagon-like peptide 1 derivative liraglutide (NN2211) markedly improves 24-h glycemia and alpha- and beta-cell function and reduces endogenous glucose release in patients with type 2 diabetes. Diabetes 53(5):1187–1194.
74. Yasuda H. 2008. Solid tumor physiology and hypoxia-induced chemo/radio-resistance: Novel strategy for cancer therapy: Nitric oxide donor as a therapeutic enhancer. Nitric Oxide 19(2):205–216.
75. Yasuda H, Yamaya M, Nakayama K, Sasaki T, Ebihara S, Kanda A, Asada M, Inoue D, Suzuki T, Okazaki T, Takahashi H, Yoshida M, Kaneta T, Ishizawa K, Yamanda S, Tomita N, Yamasaki M, Kikuchi A, Kubo H, Sasaki H. 2006. Randomized phase II trial comparing nitroglycerin plus vinorelbine and cisplatin with vinorelbine and cisplatin alone in previously untreated stage IIIB/IV non-small-cell lung cancer. J Clin Oncol 24(4):688–694.
76. Hogg N. 2000. Biological chemistry and clinical potential of S-nitrosothiols. Free Radic Biol Med 28(10):1478–1486.
77. Hryniuk WM, Figueredo A, Goodyear M. 1987. Applications of dose intensity to problems in chemotherapy of breast and colorectal cancer. Semin Oncol 14(4 Suppl 4):3–11.
78. Wallace JL, Del Soldato P. 2003. The therapeutic potential of NO-NSAIDs. Fundam Clin Pharmacol 17(1):11–20.
79. Marley R, Feelisch M, Holt S, Moore K. 2000. A chemiluminescense-based assay for S-nitrosoalbumin and other plasma S-nitrosothiols. Free Radic Res 32(1):1–9.
80. Ishima Y, Akaike T, Kragh-Hansen U, Hiroyama S, Sawa T, Suenaga A, Maruyama T, Kai T, Otagiri M. 2008. S-nitrosylated human serum albumin-mediated cytoprotective activity is enhanced by fatty acid binding. J Biol Chem 283(50):34966–34975.
81. Katayama N, Nakajou K, Ishima Y, Ikuta S, Yokoe J, Yoshida F, Suenaga A, Maruyama T, Kai T, Otagiri M. 2010. Nitrosylated human serum albumin (SNO-HSA) induces apoptosis in tumor cells. Nitric Oxide 22(4):259–265.
82. Katayama N, Nakajou K, Komori H, Uchida K, Yokoe J, Yasui N, Yamamoto H, Kai T, Sato M, Nakagawa T, Takeya M, Maruyama T, Otagiri M. 2008. Design and evaluation of S-nitrosylated human serum albumin as a novel anticancer drug. J Pharmacol Exp Ther 325(1):69–76.
83. Maeda H, Wu J, Sawa T, Matsumura Y, Hori K. 2000. Tumor vascular permeability and the EPR effect in macromolecular therapeutics: A review. J Control Release 65(1–2):271–284.
84. Tanaka T, Shiramoto S, Miyashita M, Fujishima Y, Kaneo Y. 2004. Tumor targeting based on the effect of enhanced permeability and retention (EPR) and the mechanism of receptor-mediated endocytosis (RME). Int J Pharm 277(1–2):39–61.
85. Seki T, Fang J, Maeda H. 2009. Enhanced delivery of macromolecular antitumor drugs to tumors by nitroglycerin application. Cancer Sci 100(12):2426–2430.
86. Adhikary S, Eilers M. 2005. Transcriptional regulation and transformation by Myc proteins. Nat Rev Mol Cell Biol 6(8):635–645.
87. Frederiksen LJ, Sullivan R, Maxwell LR, Macdonald-Goodfellow SK, Adams MA, Bennett BM, Siemens DR, Graham CH. 2007. Chemosensitization of cancer in vitro and in vivo by nitric oxide signaling. Clin Cancer Res 13(7):2199–2206.
88. Jordan BF, Beghein N, Aubry M, Gregoire V, Gallez B. 2003. Potentiation of radiation-induced regrowth delay by isosorbide dinitrate in FSaII murine tumors. Int J Cancer 103(1):138–141.
89. Wink DA, Cook JA, Christodoulou D, Krishna MC, Pacelli R, Kim S, DeGraff W, Gamson J, Vodovotz Y, Russo A, Mitchell JB. 1997. Nitric oxide and some nitric oxide donor compounds enhance the cytotoxicity of cisplatin. Nitric Oxide 1(1):88–94.
90. Chen JY, Scerbo M, Kramer G. 2009. A review of blood substitutes: Examining the history, clinical trial results, and ethics of hemoglobin-based oxygen carriers. Clinics (Sao Paulo) 64(8):803–813.
91. Jahr JS, Moallempour M, Lim JC. 2008. HBOC-201, hemoglobin glutamer-250 (bovine), Hemopure (Biopure Corporation). Expert Opin Biol Ther 8(9):1425–1433.

92. Sakai H, Sou K, Horinouchi H, Kobayashi K, Tsuchida E. 2009. Review of hemoglobin-vesicles as artificial oxygen carriers. Artif Organs 33(2):139–145.
93. Smani Y. 2008. Hemospan: A hemoglobin-based oxygen carrier for potential use as a blood substitute and for the potential treatment of critical limb ischemia. Curr Opin Investig Drugs 9(9):1009–1019.
94. Lok C. 2001. Blood product from cattle wins approval for use in humans. Nature 410(6831):855.
95. Tsuchida E, Ando K, Maejima H, Kawai N, Komatsu T, Takeoka S, Nishide H. 1997. Properties of and oxygen binding by albumin–tetraphenylporphyrinatoiron(II) derivative complexes. Bioconjug Chem 8(4):534–538.
96. Komatsu T, Matsukawa Y, Tsuchida E. 2002. Effect of heme structure on O(2)-binding properties of human serum albumin–heme hybrids: Intramolecular histidine coordination provides a stable O(2)-adduct complex. Bioconjug Chem 13(3):397–402.
97. Tsuchida E, Komatsu T, Matsukawa Y, Hamamatsu K, Wu J. 1999. Human serum albumin incorporating tetrakis(o-pivalamido) phenylporphinatoiron(II) derivative as a totally synthetic O_2-carrying hemoprotein. Bioconjug Chem 10(5):797–802.
98. Huang Y, Komatsu T, Nakagawa A, Tsuchida E, Kobayashi S. 2003. Compatibility in vitro of albumin–heme (O(2) carrier) with blood cell components. J Biomed Mater Res A 66(2):292–297.
99. Tsuchida E, Komatsu T, Matsukawa Y, Nakagawa A, Sakai H, Kobayashi K, Suematsu M. 2003. Human serum albumin incorporating synthetic heme: Red blood cell substitute without hypertension by nitric oxide scavenging. J Biomed Mater Res A 64(2):257–261.
100. Komatsu T, Yamamoto H, Huang Y, Horinouchi H, Kobayashi K, Tsuchida E. 2004. Exchange transfusion with synthetic oxygen-carrying plasma protein "albumin–heme" into an acute anemia rat model after seventy-percent hemodilution. J Biomed Mater Res A 71(4):644–651.
101. Tsuchida E, Komatsu T, Hamamatsu K, Matsukawa Y, Tajima A, Yoshizu A, Izumi Y, Kobayashi K. 2000. Exchange transfusion with albumin–heme as an artificial O_2-infusion into anesthetized rats: Physiological responses, O_2-delivery, and reduction of the oxidized hemin sites by red blood cells. Bioconjug Chem 11(1):46–50.
102. Horinouchi H, Yamamoto H, Komatsu T, Huang Y, Tsuchida E, Kobayashi K. 2008. Enhanced radiation response of a solid tumor with the artificial oxygen carrier 'albumin–heme'. Cancer Sci 99(6):1274–1278.
103. Kobayashi K, Komatsu T, Iwamaru A, Matsukawa Y, Horinouchi H, Watanabe M, Tsuchida E. 2003. Oxygenation of hypoxic region in solid tumor by administration of human serum albumin incorporating synthetic hemes. J Biomed Mater Res A 64(1):48–51.

Bioconjugate Chemistry

Article

pubs.acs.org/bc

S-Nitrosated Human Serum Albumin Dimer is not only a Novel Anti-Tumor Drug but also a Potentiator for Anti-Tumor Drugs with Augmented EPR Effects

Yu Ishima,[†,‡] Di Chen,[†] Jun Fang,[§,#] Hiroshi Maeda,[#] Ai Minomo,[†] Ulrich Kragh-Hansen,[¶] Toshiya Kai,[†,∥] Toru Maruyama,[†,‡] and Masaki Otagiri*[,†,§,#]

[†]Department of Biopharmaceutics, Graduate School of Pharmaceutical Sciences, and [‡]Center for Clinical Pharmaceutical Science, Kumamoto University, 5-1 Oe-honmachi, Kumamoto 862-0973, Japan

[§]Faculty of Pharmaceutical Sciences and [#]Drug Delivery System Research Institute, Sojo University, 4-22-1 Ikeda, Kumamoto 860-0082, Japan

[¶]Department of Medical Biochemistry, University of Aarhus, DK-8000 Aarhus C, Denmark

[∥]Tohoku Nipro Pharmaceutical Corporation, 428 Okanouchi, Kagamiishimachi, Iwasegun, Fukushima 969-0401, Japan

Supporting Information

ABSTRACT: Macromolecules have been developed as carriers of low-molecular-weight drugs in drug delivery systems (DDS) to improve their pharmacokinetic profile or to promote their uptake in tumor tissue via enhanced permeability and retention (EPR) effects. In the present study, recombinant human serum albumin dimer (AL-Dimer), which was designed by linking two human serum albumin (HSA) molecules with the amino acid linker $(GGGGS)_2$, significantly accumulated in tumor tissue even more than HSA Monomer (AL-Monomer) and appearing to have good retention in circulating blood in murine colon 26 (C26) tumor-bearing mice. Moreover, we developed *S*-nitrosated AL-Dimer (SNO-AL-Dimer) as a novel DDS compound containing AL-Dimer as a carrier, and nitric oxide (NO) as (i) an anticancer therapeutic drug/cell death inducer and (ii) an enhancer of the EPR effect. We observed that SNO-AL-Dimer treatment induced apoptosis of C26 tumor cells *in vitro*, depending on the concentration of NO. In *in vivo* experiments, SNO-AL-Dimer was found to specifically deliver large amounts of cytotoxic NO into tumor tissue but not into normal organs in C26 tumor-bearing mice as compared with control (untreated tumor-bearing mice) and SNO-AL-Monomer-treated mice. Intriguingly, *S*-nitrosation improved the uptake of AL-Dimer in tumor tissue through augmenting the EPR effect. These data suggest that SNO-AL-Dimer behaves not only as an anticancer therapeutic drug, but also as a potentiator of the EPR effect. Therefore, SNO-AL-Dimer would be a very appealing carrier for utilization of the EPR effect in future development of cancer therapeutics.

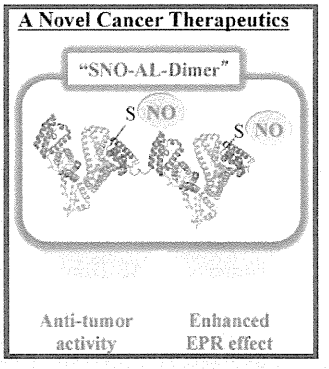

INTRODUCTION

Lack of efficiency in delivering therapeutic agents to a target tumor region leading to severe toxic side effects is most often a barrier to the clinical application of novel therapeutic anticancer drugs in cancer therapy. To limit the side effects of cancer chemotherapy, drug delivery systems (DDS) are being developed with specific targeting for cancers and increased retention in tumor tissues,[1−3] and/or to enhance the stability and half-life of low-molecular-weight drugs such as nitric oxide (NO) in the circulation.[4] Previous reports have shown that macromolecules such as human serum albumin (HSA) and synthetic polymers seem to be useful as carriers of low-molecular-weight drugs in DDS systems to improve the pharmacokinetic profile of the drugs or to promote the uptake of drugs in tumor tissue via enhanced permeability and retention (EPR) effects.[5−7] These findings have inspired research toward the development of DDS with specific targeting potential for tumor tissues in cancer therapy.

NO has been reported to cause DNA damage and direct cell death at high concentrations.[8,9] Therefore, it has been realized that NO has potential for cancer therapy, and it is emerging as an antioncogenic agent which, in contrast to conventional therapeutic agents,[10,11] is able to overcome the often-seen tumor cell resistance to treatment. Although there are several NO donors, such as *S*-nitrosoglutathione (GSNO) and NO-donating nonsteroidal anti-inflammatory drugs (NO-NSAIDs), which were shown to induce apoptosis of tumor cells *in vitro*,[12,13] their clinical use is limited by some problems, such as toxicity at high concentrations due to lack of specificity for tumor cells or side effects occurring during long-term application.[14−16] As a consequence, binding of NO to a

Received: September 29, 2011
Revised: November 23, 2011
Published: January 7, 2012

potential carrier to form a stable NO-releasing DDS is proposed as an approach that would overcome these problems.

Recombinant human serum albumin dimer (AL-Dimer), in which the C-terminus of one HSA molecule was linked to the N-terminus of another HSA molecule by the amino acid linker $(GGGGS)_2$, was designed and successfully produced by the yeast *Pichia pastoris*. It has been reported that AL-Dimer has a longer circulation time than the monomeric form of HSA (AL-Momomer).[17] Because of that finding, we presumed that AL-Dimer would be a good candidate to improve the pharmacokinetic profile of a low-molecular-weight drug such as NO which otherwise has a very short plasma half-life *in vivo*. Moreover, AL-Dimer is expected to have an enhanced accumulation in solid tumor via the EPR mechanism[18,19] due to its large molecular weight (130 kDa). Therefore, it is possible that AL-Dimer could be of great clinical use as a new DDS material with a superior plasma retention property (e.g, prolonged plasma half-life) as well as with increased tumor specific accumulation.

In this study, we developed a novel DDS system of NO, a potential anticancer therapeutic, using AL-Dimer as a carrier, namely, *S*-nitrosated AL-Dimer (SNO-AL-Dimer), and examined its physicochemical properties. Then, the biodistribution and anticancer ability of SNO-AL-Dimer was evaluated both *in vitro* in murine colon 26 (C26) tumor cells and *in vivo* in C26 tumor-bearing mice. In addition, we also investigated whether SNO-AL-Dimer enhanced the EPR effect by delivering NO.

EXPERIMENTAL PROCEDURES

Chemicals. AL-Monomer and AL-Dimer were synthesized using the yeast *Pichia pastoris* (*P. pastoris*) (strain GS115).[17] AL-Monomer and AL-Dimer were defatted by means of a charcoal treatment as described by Chen.[20] Sephadex G-25 (φ 1.6 × 2.5 cm) was from GE Healthcare (Kyoto, Japan). *S*-Nitrosoglutathione (GSNO) was purchased from Dojindo Laboratories (Kumamoto, Japan). 1,4-Dithiothreitol (DTT) was from Sigma-Aldrich (St. Louis, MO). Isoamyl nitrite (IAN) was bought from Wako Chemicals (Osaka, Japan). Diethylenetriaminepentaacetic acid (DTPA) and EDTA were purchased from Nacalai Tesque (Kyoto, Japan). $^{111}InCl_3$ was a gift from Nihon Medi-Physics Co., Ltd. (Hyogo, Japan).

Cells and Animals. C26 cells were cultured in RPMI-1640 containing 10% fetal bovine serum (San kou junyaku, Co., Ltd., Japan), 100 units/mL penicillin, and 100 μg/mL streptomycin, incubated in a humidified (37 °C, 5% CO_2 and 95% air) incubator, grown in 75 cm^2 flask (Falcon BD), and passaged when 75% confluency was reached. Male BALB/cAnNCrlCrlj mice (5 weeks old, 17–22 g) were purchased from Charles River Laboratories, Japan. A C26 solid tumor model was established by subcutaneously implanting of 1×10^6 C26 cells into the back of the mice.

Synthesis of SNO-HSAs. SNO-HSAs were prepared according to a previous report.[21] In brief, the HSA forms (20 mg/mL) were incubated with 3 mM DTT for 5 min at 37 °C. Afterward, the DTT was removed quickly by Sephadex G-25 gel filtration and eluted with 0.1 M potassium phosphate buffer (pH 7.4) containing 0.5 mM DTPA. DTT-treated HSAs (20 mg/mL) were incubated with 3 mM isoamyl nitrite (IAN) for 60 min protected from light at 37 °C. SNO-HSAs were purified by Sephadex G-25 gel filtration, eluted with phosphate buffered saline (PBS) (pH 7.4). These samples were stored at −80 °C until used in the experiments.

Physicochemical Characterization of HSAs. *CD Spectra.* Circular dichrosim (CD) spectra of AL-Monomer and AL-Dimer were measured using J-720-type spectropolarimeter (JASCO, Tokyo, Japan). For the calculation of mean residue ellipticity [θ], the molecular weight was considered as 66.5 kDa for AL-Monomer and 130 kDa for AL-Dimer.[17]

Capillary Zone Electrophoresis. The P/ACE MDQ system (Beckman Instruments, Fullerton, CA, USA) in conjunction with a photodiode array detector was employed to determine the net charge of AL-Dimer compared with AL-Monomer. Capillaries with total capillary length of 60 cm (50 cm to the detector) were used. New capillaries were initialized by flushing with water (5 min), 0.1 M NaOH (5 min), water (5 min), and run buffer (5 min) before use. Between analyses the capillary was rinsed with 0.1 M NaOH (3 min), water (3 min), and run buffer (3 min). Injection was performed at a pressure of 0.5 psi for 5 s, and detection was performed at a wavelength of 214 nm.

SDS-PAGE. The purity of AL-Monomer and AL-Dimer was examined by 8% reduced sodium dodecyl sulfate polyacrylamide gel electrophoresis (SDS-PAGE). Gross conformational changes induced by *S*-nitrosation of AL-Monomer and AL-Dimer were assessed by means of nonreducing SDS-PAGE (8%) at 4 °C in the dark. The bands were stained by using Coomassie Brilliant Blue (CBB).

Anti-Oxidant Activity of HSAs. For 1,1′-diphenyl-2-picrylhydrazyl (DPPH) radicals, the radical scavenging activity of the HSAs (0.67 mg/mL; AL-Monomer 10 μM; AL-Dimer 5 μM) was determined from the decrease in the absorbance of DPPH radicals at 517 nm due to their scavenging of an unpaired electron of the stable DPPH radical in a mixture of 10 mL ethanol, 10 mL of 50 mM 2-(*N*-morpholino)ethanesulfonic acid (Mes) buffer (pH 5.5), and 5 mL of 0.5 mM DPPH in ethanol.[22] For $O_2^{\bullet-}$, the xanthine/xanthine oxidase (X/XO) system was used to generate $O_2^{\bullet-}$ to measure the superoxide-scavenging activity of the HSAs. Briefly, 1 mL of solution contained 100 μg/mL X, 0.01 U/mL XO, 250 μM DTPA, and 500 μM luminol in the absence or presence of 0.67 ng/mL of HSAs (AL-Monomer 10 nM; AL-Dimer 5 nM). The chemiluminescence (CL) response was continuously recorded for 4 min at room temperature using Mini Lumat LB 9506 luminometer (EG&G Berthold, Germany). CL was obtained from the slope of the counts versus the time graph. To evaluate the NO scavenging activity of the HSAs, we measured the amount of the *S*-nitroso moiety of HSAs after incubation with NO by means of HPLC coupled with a flow reactor assay, as previously reported.[23] Briefly, 10 mg/mL HSAs (AL-Monomer 150 μM; AL-Dimer 75 μM) was incubated with 5 mM NOC7 for 10 min in PBS at 25 °C in the dark. To stop the reaction, 1.5 mM *N*-ethylmaleimide was added to these reaction solutions; the resulting solutions were kept at −80 °C until analysis.

Determination of SNO-Moiety and Stability of SNO-HSAs. The amounts of the SNO-moiety of the SNO-HSAs were quantified by HPLC coupled with a flow reactor system, as previously reported.[23] The stability of the SNO-moiety on storage was examined as follows. SNO-HSAs were dissolved in PBS with 0.5 mM DTPA (pH 7.4) and protected from light at 4 or 25 °C. At appropriate times after the start of incubation, aliquots of the SNO-HSA solutions were taken, and the SNO-moieties were determined by HPLC as mentioned above.

Pharmacokinetic Experiments. The HSAs and SNO-HSAs were labeled with ^{111}In by using DTPA anhydride as a

dx.doi.org/10.1021/bc2005363 | *Bioconjugate Chem.* 2012, 23, 264–271

bifunctional chelating agent.[24,25] The pharmacokinetics and body distribution of HSAs and SNO-HSAs were carried out in a C26 solid tumor model. In brief, ^{111}In-labeled protein was dissolved in saline, and the concentration of ^{111}In-labeled protein was adjusted by addition of nonradiolabeled protein to the solution. The ^{111}In-labeled protein solution was administrated intravenously via the tail vein at a dose of 1 mg/kg. At scheduled times after the intravenous injection, the mice were sacrificed, and blood was collected from the inferior vena cava. Tumor tissue was collected for tumor distribution. The radioactivity of each sample was counted using a well-type NaI scintillation counter ARC-2000 (Aloka, Tokyo, Japan).

Cell Death Induced by the HSAs. For detection of C26 cell death induced by the HSAs with and without *S*-nitrosation, the cells were seeded in flat-bottomed 96-well plates (1×10^4 cells per well). After culturing for 21 h, the media were refreshed and HSAs with different NO concentrations were added into the plates. After further 24 h, cell death was evaluated by the lactate dehydrogenase (LDH) assay from Wako Pure Chemical (Osaka, Japan). The percentage of dead cells was determined using the following formula: $(T - L)/(H - L) \times 100$, where T is the absorbance at 490 nm of supernatants of HSA-treated cells, using 630 nm as a reference, L is the absorbance of supernatants of control untreated cells, and H is the absorbance corresponding to the maximal (100%) LDH release of Triton-lysed cells.

In Vivo Measurement of NOx. C26 tumor-bearing mice were produced with the method mentioned above. 100 μL SNO-AL-Dimer, SNO-AL-Monomer, or GSNO were administrated intravenously via the tail vein at dose of 1.3 μmol NO/kg. At 6 h after the intravenous injection, the mice were sacrificed, and blood was collected from inferior vena cava, followed by collection of tumors as well as normal tissues, i.e., liver and kidney. The collected blood was centrifuged, and 100 μL of plasma was used for this study. The tumor and normal tissues were homogenized by use of BioMashaer. NO*x* (NO_2^- + NO_3^-) level was measured by the HPLC flow-reactor system, and NO*x*, the oxidative metabolites of NO, were quantified by the Griess reaction.

Effect of SNO-HSAs on Solid Tumor Vascular Permeability. C26 tumors obtained from at least six mice per group at 10 days after tumor cell inoculation were used for the *in vivo* vascular permeability experiments, as previously reported.[26] SNO-AL-Monomer and SNO-AL-Dimer were administered i.v. via the tail vein at doses of 1.3 μmol NO/kg. To assess vascular permeability in solid tumors, Evans blue dye that binds to serum albumin quickly *in vivo* to behave as a macromolecule was injected i.v. at a dose of 10 mg/kg into the tumor-bearing mice at 6 h after administration of the SNO-HSAs. At 24 h after the Evans blue dye injection, the dye in the solid tumor was extracted with formamide and quantified by UV absorption at 620 nm, as described previously.[5]

Statistical Analysis. The statistical significance of collected data was evaluated using the ANOVA analysis followed by Newman-Keuls method for more than 2 means. Differences between the groups were evaluated by Student's *t* test. $P < 0.05$ was regarded as statistically significant.

RESULTS AND DISCUSSION

Physicochemical and Structural Properties of AL-Dimer Compared with AL-Monomer. Physicochemical properties of macromolecular carriers including molecular weight and electric charge influence their biological properties, such as plasma half-life, tumor accumulation, and tumor cell uptake which are important factors for tumor targeted carriers.[27] Therefore, we examined the physicochemical and structural properties of AL-Dimer. First, SDS-PAGE was used to evaluate the molecular weight and purity of AL-Dimer generated by the *P. pastoris* system. From Figure 1A, it is seen

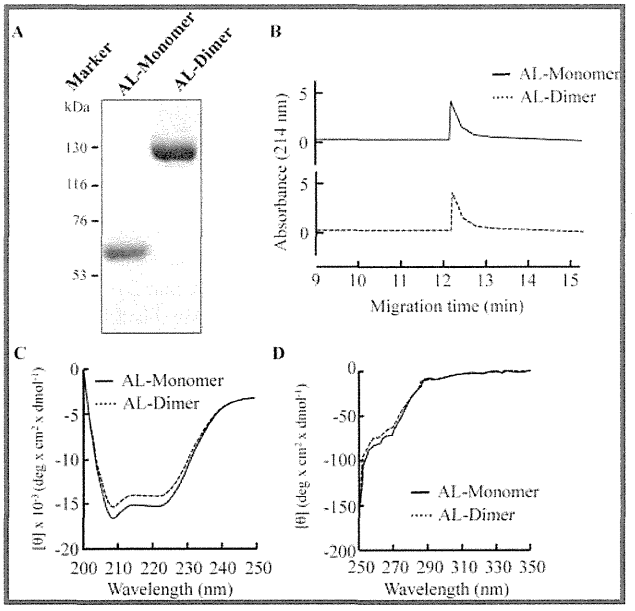

Figure 1. (A) Reduced SDS-PAGE (8%) of AL-Monomer and AL-Dimer visualized by CBB staining. (B) Capillary zone electrophoresis examination of AL-Monomer and AL-Dimer (both at a concentration of 10 mg/mL) in PBS (pH 7.4) solution. Far-UV (C) and near-UV (D) CD spectra of AL-Monomer and AL-Dimer in PBS (pH 7.4) solution at 25 °C.

that under reducing conditions AL-Dimer shows as a single band with a molecular mass of 130 kDa, which is approximately twice the molecular weight of AL-Monomer. This finding indicates a successful generation of pure AL-Dimer. The net charge of HSA was not modified by dimerization, because capillary zone electrophoresis shows that the net charge related to the amount of protein is the same for AL-Dimer and AL-Monomer (Figure 1B). The conformational structure of the two albumin forms were evaluated by CD spectra. As shown in Figure 1C and D, AL-Dimer has CD spectra which are only slightly different from those of AL-Monomer. These results suggest that AL-Dimer has a conformational structure similar to that of AL-Monomer. Furthermore, we checked the effect of AL-Dimerization on the accessibility of ^{34}Cys using DTNB, and as seen from Table 1, dimerization of HSA did not affect the accessibility of ^{34}Cys. Finally, we studied the scavenging activity of the two albumin forms against three different ROS, namely, DPPH, $O_2^{\bullet-}$, and NO (Table 1). In all three examples, AL-Dimer has a significantly higher scavenging activity than AL-Monomer, suggesting small but facilitating changes in the microenvironment of other antioxidative amino acid residues in AL-Dimer than ^{34}Cys (Figure 1C and D).

Physicochemical Properties of SNO-AL-Dimer Compared with SNO-AL-Monomer. Nonreducing SDS-PAGE was used to confirm the purity of SNO-AL-Dimer after *S*-nitrosation reaction (Supporting Information Figure 1). It revealed only a single band for SNO-AL-Dimer with the same

Table 1. Physicochemical Characterization of AL-Monomer and AL-Dimer

	Number of free Cysteine (mol SH/mol protein)	SH accessibility to DTNB[a] (A_5/A_{60}/mol SH)	radical scavenging activities (%) DPPH	$O_2^{\bullet-}$	NO
AL-Monomer	1	0.73 ± 0.08[b]	36 ± 6.4	30 ± 9.4	26 ± 8.4
AL-Dimer	2	0.68 ± 0.13	47 ± 4.4*	45 ± 8.6*	37 ± 6.6*

[a]The accessibility was evaluated as A_5/A_{60}, where A_5 and A_{60} is the sample absorbance at 405 nm after 5 and 60 min (maximal absorbency), respectively, of incubation with DTNB. [b]Results are expressed as means ± SD (n = 3–9). *P < 0.05, as compared with AL-Monomer.

Table 2. Physicochemical Characterization of SNO-AL-Monomer and SNO-AL-Dimer

	SNO moiety (mol SNO/mol protein)	half-lives ($T_{1/2}$) in PBS at 4 °C (day)	half-lives ($T_{1/2}$) in PBS at 25 °C (day)	decomposition products
SNO-AL-Monomer	0.52 ± 0.20[a]	25.4 ± 12.2	21.3 ± 7.4	AL-Monomer
SNO-AL-Dimer	1.48 ± 0.25*	46.8 ± 15.1*	39.0 ± 11.9*	AL-Dimer

[a]Results are expressed as means ± SD (n = 3–6). *P < 0.05, as compared with AL-Monomer.

molecular mass of AL-Dimer, which indicated that *S*-nitrosation did not cause dimerization of AL-Dimer via disulfide bond formation, or fragmentation or gross conformational changes of AL-Dimer. The analysis also showed no gross conformational changes in the case of *S*-nitrosation of AL-Monomer. From Table 2 it is seen that the present approach is efficient in *S*-nitrosation of the AL-Dimer, because the preparation contains on average 1.48 mol of NO per mol of protein.

We determined the stability of the two SNO-preparations in phosphate buffer protected from light. At 4 °C the apparent half-life of the SNO-moiety of SNO-AL-Dimer is about 47 days, which is significantly longer than that of the SNO-AL-Monomer (i.e., 25 days) (Table 2). Also at 25 °C, the half-lives were long, i.e., 39 and 21 days for SNO-AL-Dimer and SNO-AL-Monomer, respectively. This result provided evidence that the SNO-HSAs are fairly stable compounds in neutral buffer even at room temperature.

Accumulation of AL-Dimer in Tumor Tissue Compared with AL-Monomer. The adverse side effects of anticancer drugs, resulting from lack of specificity in conventional therapies, usually limit the increase of dose intensity which is required to eradicate the cancerous growth.[28–30] One of the developing strategies for the enhancement of tumor specific delivery of the therapeutics is albumin-based drug delivery technology.[1,31] Albumin has emerged as a drug carrier in the past 10 years for drug targeting and for improving the pharmacokinetic profile of various therapeutic drugs.[31–33] Examples are the antitumor therapeutic drug doxorubicin–albumin conjugate,[34] and the use of cationized albumin as drug carrier for blood-brain barrier transport.[35,36] In order to clarify whether intravenously injected AL-Dimer accumulate in solid tumor tissue, we performed a biodistribution analysis of AL-Dimer given to C26 tumor-bearing mice. As shown in Figure 2A, it was observed that at 24 h after injection the accumulation of AL-Dimer in the tumor tissue was 1.8 times higher than that of AL-Monomer. Moreover, AL-Dimer showed a much higher level of blood retention compared with that of AL-Monomer (Figure 2B). These findings are consistent with a previous study showing that proteins with molecular weights ranging from 12 to 150 kDa correlated with the rate of tumor uptake, and that long circulation times lead to enhanced tumor uptakes of the protein.[34] Thus, AL-Dimer seems to be a good candidate as a drug carrier, because in addition to a prolonged blood retention it has a good accumulation in tumor tissue.

Thus, the physicochemical characterization showed that AL-Dimer has a conformational structure and net charge which in principle are similar to those of AL-Monomer. Furthermore, the pharmacokinetics and biodistribution studies very importantly showed that AL-Dimer has superior blood retention properties and tumor targeting potential. Therefore, based on

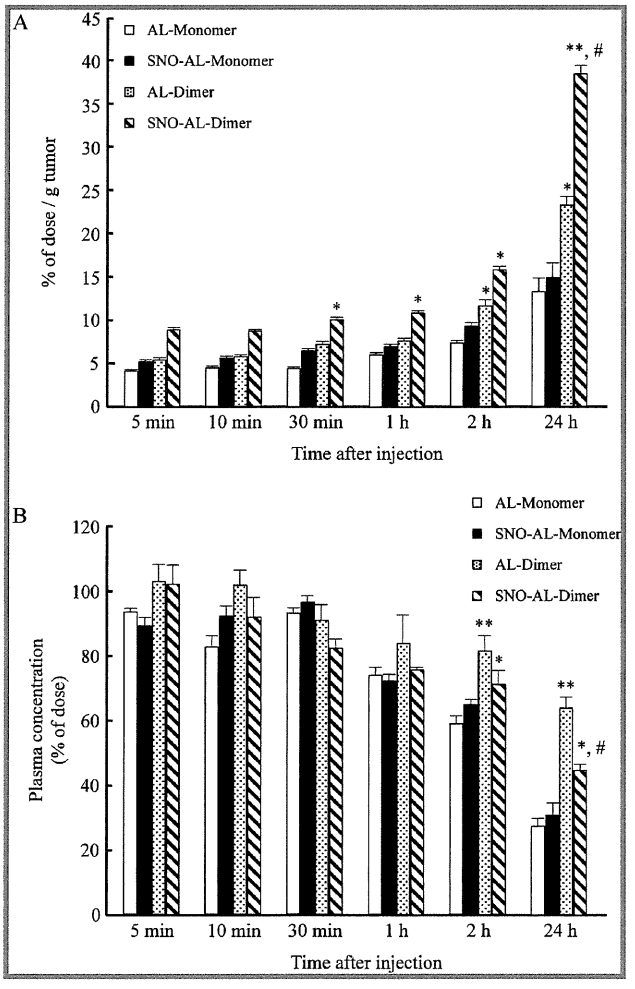

Figure 2. Tumor accumulation (A) and blood retention (B) of ^{111}In-labeled AL-Monomer and AL-Dimer with and without *S*-nitrosation after intravenous administration to C26 tumorbearing mice at a dose of 1 mg/kg. Results are means ± SD (n = 4). * P < 0.05, ** P < 0.01 compared with AL-Monomer or SNO-AL-Monomer, # P < 0.05 compared with AL-Dimer.

dx.doi.org/10.1021/bc2005363 | Bioconjugate Chem. 2012, 23, 264–271

these findings, we found that exploiting recombinant AL-Dimer as a drug carrier would have several advantages over HSA: (a) the use of commercial and possibly pathogenic albumin is avoided; (b) AL-Dimer is expected to be effective in binding albumin-binding drugs, among other things because it has two molecules of ^{34}Cys. (c) AL-Dimer could enhance the stability of therapeutic drugs both *in vitro* and *in vivo* and improve their blood retention and tumor accumulation *in vivo*. These potential advantages stimulated our attempt to utilize AL-Dimer as a carrier of antitumor therapeutic drugs and thereby to develop a new drug delivery system for cancer therapy. We chose to use NO as the potential anticancer agent and developed SNO-AL-Dimer to confirm the potential of AL-Dimer as a carrier in anticancer DDS. First, for evaluating whether *S*-nitrosation of AL-Dimer changes its pharmacokinetic parameters, we performed a biodistribution analysis of SNO-AL-Dimer in C26 tumor-bearing mice. Promisingly, the results showed that the accumulation of SNO-AL-Dimer in tumor tissue was 2.6 and 1.6 times higher than that of SNO-AL-Monomer and AL-Dimer, respectively, suggesting that *S*-nitrosation of AL-Dimer further enhanced its EPR effect, probably via NO release from SNO-AL-Dimer.

C26 Tumor Cell Death Induced by SNO-AL-Dimer Compared with SNO-AL-Monomer. C26 tumor cells were used for investigating the cytotoxicity of different albumin preparations, and cell death was assayed by the quantification of extracelluar LDH release. As shown in Figure 3A, both AL-Dimer and AL-Monomer have a small cytotoxic effect, i.e., only about 10% of the cells were dead after 24 h of exposure to 20 mg protein/mL. By contrast, SNO-AL-Dimer or SNO-AL-Monomer treatment resulted in a much more pronounced LDH release from the cells and in a NO-dose dependent manner, i.e., 70% or more of the cells died in the presence of 80 μM of SNO (Figure 3B). This result is in agreement with a previous study which reports that NO donors such as sodium nitroprusside (SNP) caused cell death depending on the NO concentration.[12] Importantly, the present findings clearly proved that NO, but not AL-Dimer, is the tumor cell death inducer, thus suggesting that AL-Dimer is a suitable carrier for anticancer drugs such as NO. Accordingly, we considered that SNO-AL-Dimer may become a new NO donor with superior pharmacological (cytotoxic) effect. Further, because of the significantly improved *in vivo* pharmacokinetics of SNO-AL-Dimer as described above, it is reasonable to expect that SNO-AL-Dimer would show a much improved antitumor effect, as well as a substantial reduction of the toxicity profile compared with traditional NO donors which are known to cause adverse side effects at high concentrations during long-term treatment.[14,15] The data obtained so far led us to perform the following *in vivo* experiments.

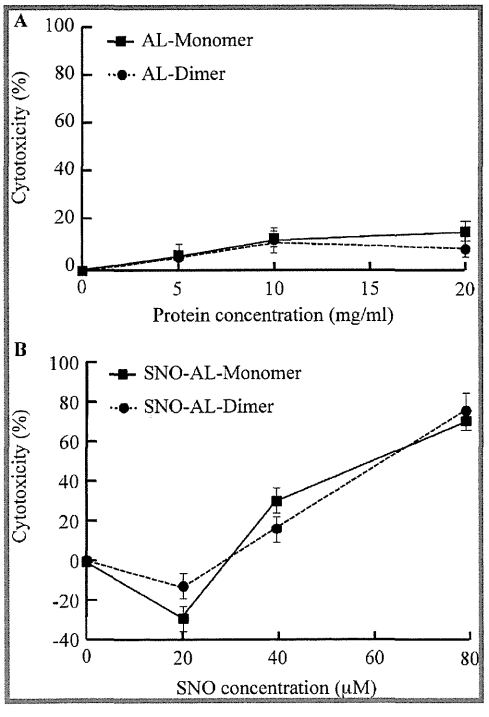

Figure 3. Cytotoxity of AL-Dimer and AL-Monomer without (A) and with (B) *S*-nitrosation. C26 cells were cultured at a density of 1×10^4 cells/well for 21 h in RPMI1640 supplemented with 10% FBS. After that period of time the medium was refreshed with AL-Dimer, AL-Monomer, SNO-AL-Dimer, or SNO-AL-Monomer for 24 h, and cell death was assessed by measurement of extracellular LDH activity. In (B), the protein concentrations were approximately 2–9 mg/mL. Results are means ± SD (n = 3–5).

NO Delivery by SNO-AL-Dimer for Tumor Targeting. To evaluate whether AL-Dimer successfully delivers NO to tumor tissue *in vivo*, a C26 solid tumor model was utilized, and the delivery of NO into tumor tissue by SNO-AL-Dimer was determined by quantification of NOx level in the tumor and compared with those of SNO-AL-Monomer and the commercially available NO donor GSNO. From Figure 4A it can be seen that intravenous treatment with SNO-AL-Dimer, but not with SNO-AL-Monomer or GSNO, caused a significant increase in the tumor level of NOx. By contrast, none of the

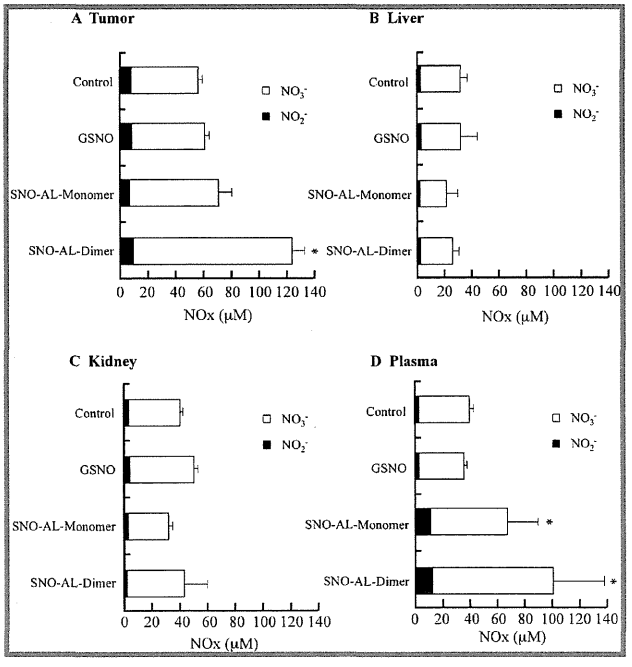

Figure 4. NOx levels in tumor tissue (A), liver (B), kidney (C), and plasma (D) at 6 h after administration of GSNO, SNO-AL-Monomer, or SNO-AL-Dimer (40 nmol NO/mouse) were determined by the HPLC flow-reactor system. Controls were mice which had not been treated with a NO-containing compound. Results are means ± SD (n = 3–11). * $P < 0.05$ compared with control.

dx.doi.org/10.1021/bc2005363 | *Bioconjugate Chem.* 2012, 23, 264–271

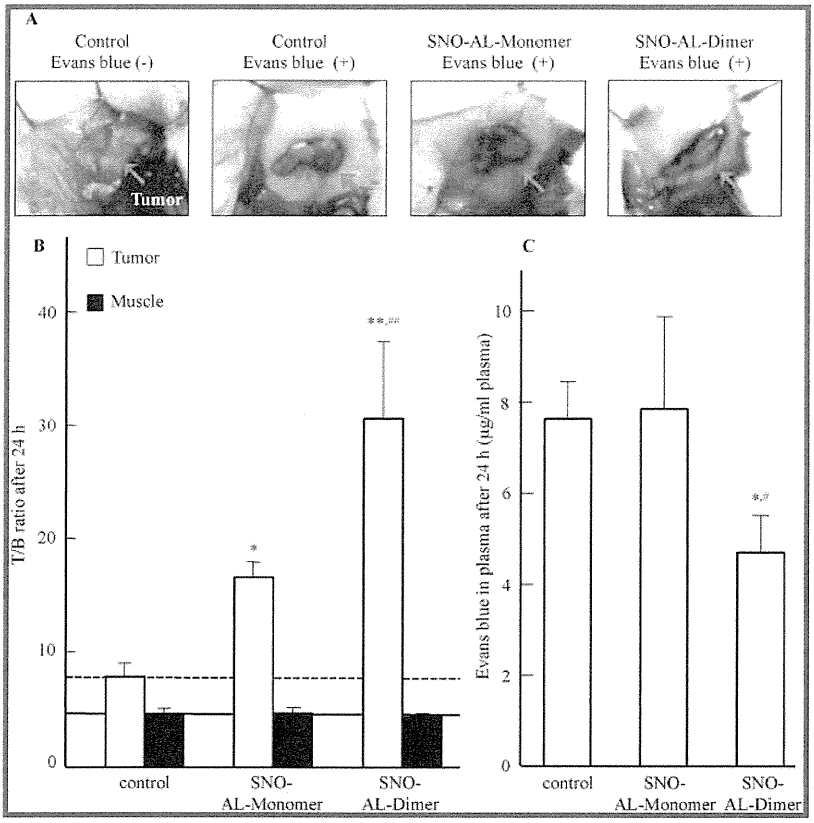

Figure 5. Extravasation of Evans blue induced by SNO-AL-Monomer and SNO-AL-Dimer. 1 $\times 10^6$ C26 cells were subcutaneously inoculated into the dorsal skin. The mice were kept for 10 days until the tumor had reached a certain volume. (A) After 10 days, saline (controls), SNO-AL-Monomer (40 nmol NO/mouse) or SNO-AL-Dimer (40 nmol NO/mouse) was injected intravenously. Six hours after administration of the different solutes, Evans blue dye was injected i.v. at a dose of 10 mg/kg into three of the four groups of the tumor-bearing mice. Twenty-four hours later, the mice were assessed. (B) Tissue–blood ratio at 24 h after intravenous injection of Evans blue dye in the C26 tumor-bearing mice. (C) Plasma concentrations of Evans blue in the mice at 24 h after i.v. injection. Results are means ± SD (n = 6–8). * $P < 0.05$, ** $P < 0.01$ compared with control, # $P < 0.05$, ## $P < 0.01$ compared with SNO-AL-Monomer.

preparations induced increased NOx levels in other organs such as liver (Figure 4B) or kidney (Figure 4C). Finally, especially SNO-AL-Dimer has a high level of blood retention (Figure 4D). These results showed that SNO-AL-Dimer is more efficient for tumor delivery of NO than a traditional NO donor such as GSNO. The findings also showed that SNO-AL-Dimer caused a much higher concentration of NOx in the tumor than SNO-AL-Monomer which has been proven as a novel anticancer drug. This may be due to the possibility that SNO–^{34}Cys is relatively stable and effective in providing a steady-state NO level *in vivo* compared with other sites binding to NO.[21]

EPR Effect was Enhanced by NO Released from SNO-AL-Dimer. To evaluate whether SNO-AL-Dimer enhances the EPR effect by delivering NO, the extravasation of Evans blue in the tumor tissue after treatment with SNO-AL-Dimer was determined, compared with SNO-AL-Monomer, using the C26 tumor-bearing mice as *in vivo* model (Figure 5A). Figure 2 shows that the accumulation of SNO-AL-Dimer in tumor tissue is 2.6 times higher than that of SNO-AL-Monomer, suggesting that S-nitrosation of AL-Dimer further enhanced its EPR effect. This enhanced effect on EPR is a most important finding in our study, and we used the Evans blue method to confirm it. Evans blue dye binds to albumin noncovalently *in vivo* after i.v. injection, and the albumin–dye complex (molecular mass of ca. 70 kDa) is extravasated in the tumor tissue due to the EPR effect. Thus, extravasation of Evans blue dye is considered to be a marker for the EPR effect of macromolecules in solid tumor.[26] Figure 5B shows that the extravasation of Evans blue dye in tumor tissue, but not in normal tissue (i.e., muscle), was significantly increased by intravenous treatment of both SNO-AL-Dimer and SNO-AL-Monomer. However, SNO-AL-Dimer induced more extravasation of Evans blue than SNO-AL-Monomer, suggesting that SNO-AL-Dimer enhances EPR effect in a much more pronounced manner, probably due to the significantly increased tumor delivery of NO from SNO-AL-Dimer as described above. In accordance with that proposal, Figure 5C shows that the plasma concentration of Evans blue after 24 h of injection is much lower in the presence of SNO-AL-Dimer than in the presence of SNO-AL-Monomer.

It has been reported by Yasuda[10] and Seki et al.[37] that the EPR effect can also be enhanced by, i.e., applying nitroglycerin (NG) ointment on the skin of tumor-bearing animals. Therefore, we compared the potential of SNO-AL-Dimer and NG on augmentation of the EPR effect. As the result, both the NOx level in tumor tissue (Supporting Information Figure 2) and the extravasation of Evans blue (Supporting Information Figure 3) are 2-fold higher in the animals given SNO-AL-Dimer than in the animals treated with NG. In light of these results, we propose that SNO-AL-Dimer possesses a powerful EPR effect. To elaborate this idea further, it is necessary to investigate the effect of SNO-AL-Dimer on the tumor

dx.doi.org/10.1021/bc2005363 | *Bioconjugate Chem.* 2012, 23, 264–271

accumulation and antitumor activity of other anticancer drugs such as Doxil or Abraxane. Our drug delivery system is also open for linking SNO-AL-Dimer to human antitumor protein toxins such as human RNase, tBID (truncated BH3-interacting domain death agonist), granzyme B, and AIF (apoptosis-inducing factor). The facile production and broad applicability make our drug delivery system a viable vehicle for anticancer drugs.

Conclusion. Our study had three major findings. First, SNO-AL-Dimer can accumulate in tumor tissue (Figure 2). Second, SNO-AL-Dimer delivers NO selectively to tumor tissue, resulting in cytotoxicity to the tumor cells (Figure 3 and Figure 4). Third, SNO-AL-Dimer behaves as a powerful enhancer of the EPR effect via NO release in the tumor (Figure 5). These findings lead to the idea that SNO-AL-Dimer possesses the clinical possibility for being not only an anticancer drug, but also a valuable tumor targeting delivery system due to enhancement of the EPR effect. In addition, we thus believe that using SNO-AL-Dimer as a carrier of anticancer drugs might be expected to improve the therapeutic potential due to the superior blood retention properties and tumor specific accumulation.

■ ASSOCIATED CONTENT

Supporting Information

Additional experimental methods and figures as described in the text. This material is available free of charge via the Internet at http://pubs.acs.org.

■ AUTHOR INFORMATION

Corresponding Author

*Tel.: +81-96-371-4150; Fax: +81-96-362-7690; E-mail: otagirim@ph.sojo-u.ac.jp.

■ ACKNOWLEDGMENTS

This research was supported by Grant-in-Aid for Scientific Research from Japan Society for the Promotion of Science (JSPS) (KAKENHI 18390051 and 22790162). This work was in part supported by grants from the Uehara Memorial Fund. Thanks are also due to members of the Gene Technology Center in Kumamoto University for their important contributions to the experiments.

■ REFERENCES

(1) Kerr, D. J., and Los, G. (1993) Pharmacokinetic principles of locoregional chemotherapy. *Cancer Surv. 17*, 105–22.

(2) Reddy, L. H. (2005) Drug delivery to tumours: recent strategies. *J. Pharm. Pharmacol. 57*, 1231–42.

(3) Moses, M. A., Brem, H., and Langer, R. (2003) Advancing the field of drug delivery: taking aim at cancer. *Cancer Cell 4*, 337–41.

(4) Katayama, N., Nakajou, K., Komori, H., Uchida, K., Yokoe, J., Yasui, N., Yamamoto, H., Kai, T., Sato, M., Nakagawa, T., Takeya, M., Maruyama, T., and Otagiri, M. (2008) Design and evaluation of *S*-nitrosolated human serum albumin as novel anticancer drug. *J. Pharmacol. Exp. Ther. 325*, 69–76.

(5) Matsumura, Y., and Maeda, H. (1986) A new concept for macromolecular therapeutics in cancer chemotherapy: mechanism of tumoritropic accumulation of proteins and the antitumor agent smancs. *Cancer Res. 46*, 6387–92.

(6) Maeda, H., and Matsumura, Y. (1989) Tumoritropic and lymphotropic principles of macromolecular drugs. *Crit. Rev. Ther. Drug Carrier Syst. 6*, 193–210.

(7) Maeda, H., Seymour, L. W., and Miyamoto, Y. (1992) Conjugates of anticancer agents and polymers: advantages of macromolecular therapeutics in vivo. *Bioconjugate Chem. 3*, 351–62.

(8) Kiziltepe, T., Hideshima, T., Ishitsuka, K., Ocio, E. M., Raje, N., and Catley, L. (2007) JS-K, a GST-activated nitric oxide generator, induces DNA double-strand breaks, activates DNA damage response pathways, and induces apoptosis in vitro and in vivo in human multiple myeloma cells. *Blood 110*, 709–18.

(9) Ishima, Y., Yoshida, F., Kragh-Hansen, U., Watanabe, K., Katayama, N., Nakajou, K., Akaike, T., Kai, T., Maruyama, T., and Otagiri, M. (2011) Cellular uptake mechanisms and responses to NO transferred from mono- and poly-S-nitrosated human serum albumin. *Free Radic. Res. 45*, 1196–206.

(10) Yasuda, H. (2008) Solid tumor physiology and hypoxia-induced chemo/radio-resistence: Novel stragegy for cancer therapy: Nitric oxide donor as a therapeutic enhancer. *Nitric Oxide 19*, 205–16.

(11) Yasuda, H., Yamaya, M., Kubo, H., and Sasaki, H. (2006) Randomized phase II trial comparing nitroglycerin plus vinorelbine and cisplatin with vinorelbine and cisplatin alone in previously untreated stage IIIB/IV non-small cell lung cancer. *J. Clin. Oncol. 24*, 688–94.

(12) Messmer, U. K., Reimer, D. M., and Brune, B. (1996) Nitric oxide-induced apoptosis: p53-dependent and p53-indeoendent signaling pathways. *Biochem. J. 319*, 299–305.

(13) Ulrich, C. M., Bigler, J., and Potter, J. D. (2006) Non-steroidal anti-inflammatory drugs for cancer prevention: promise, perils and pharmacogenetics. *Nat. Rev. Cancer 6*, 130–40.

(14) Hryniuk, W. A., Figueredo, A., and Goodyear, M. (1987) Applications of dose intensity to problems in chemotherapy of breast and colorectal cancer. *Semin. Oncol. 11*, 3–11.

(15) Hogg, N. (2000) Biological chemistry and clinical potential of S-nitrosothiols. *Free Radic. Biol. Med. 28*, 1478–86.

(16) Wallace, J. L., Del., and Soldato, P. (2003) The therapeutic potential of NO-NSAIDs. *Fundam. Clin. Pharmacol. 17*, 11–20.

(17) Matsushita, S., Chuang, V. T., Kanazawa, M., Tanase, S., Kawai, K., Maruyama, T., Suenaga, A., and Otagiri, M. (2006) Recombinant human serum albumin dimer has high blood circulation activity and low vascular permeability in comparison with native human serum albumin. *Pharm. Res. 23*, 882–91.

(18) Maeda, H., Wu, J., Sawa, T., Matsumura, Y., and Hori, K. (2000) Tumor vascular permeability and the EPR effect in macromolecular therapeutics: a review. *J. Controlled Release 65*, 271–84.

(19) Tanaka, T., Shiramoto, S., Miyashita, M., Fujishima, Y., and Kaneo, Y. (2004) Tumor targeting based on the effect of enhanced permeability and retention and the mechanism of receptor-mediated endocytosis. *Int. J. Pharm. 227*, 39–61.

(20) Chen, R. F. (1967) Removal of fatty acids from serum albumin by charcoal treatment. *J. Biol. Chem. 242*, 173–81.

(21) Ishima, Y., Sawa, T., Kragh-Hansen, U., Miyamoto, Y., Matsushita, S., Akaike, T., and Otagiri, M. (2007) *S*-nitrosylation of human variant albumin Liprizzi (R410C) confers potent antibacterial and cytoprotective properties. *J. Pharmacol. Exp. Ther. 320*, 969–77.

(22) Sassa, H., Takaishi, Y., and Terada, H. (1990) The triterpene celastrol as a very potent inhibitor of lipid peroxidation in mitochondria. *Biochem. Biophys. Res. Commun. 172*, 890–7.

(23) Akaike, T. (2000) Mechanisms of biological *S*-nitrosation and its measurement. *Free Radic. Res. 33*, 461–9.

(24) Yamasaki, Y., Sumimoto, K., Nishikawa, M., Yamashita, F., Yamaoka, K., Hashida, M., and Takakura, Y. (2002) Pharmacokinetic analysis of in vivo disposition of succinylated proteins targeted to liver nonparenchymal cells via scavenger receptors: importance of molecular size and negative charge density for in vivo recognition by receptors. *J. Pharmacol. Exp. Ther. 301*, 467–77.

(25) Peters, T., Jr. (1996) *All about Albumin: Biochemistry, Genetics, and Medical Applications*, Academic Press, San Diego.

(26) Wu, J., Akaike, T., and Maeda, H. (1998) Modulation of enhanced vascular permeability in tumors by a bradykinin antagonist, a cyclooxygenase inhibitor, and a nitric oxide scavenger. *Cancer Res. 58*, 159–65.

(27) Dreher, M., Liu, W., Michelich, C. R., Dewhirst, M. W., Yuan, F., and Chilkoti, A. (2006) Tumor vascular permeability, Accumulation, and penetration of macromolecular drug carriers. *J. Natl. Cancer Inst. 98*, 335–44.
(28) Jain, R. K. (2001) Delivery of molecular and cellular medicine to solid tumors. *Adv. Drug Delivery Rev. 46*, 149–68.
(29) Sehouli, J., Stengel, D., Oskay, G., Camara, O., Hindenburg, H. J., Klare, P., Blohmer, J., Heinrich, G., Elling, D., Ledwon, P., Lichtenegger, W., and NOGGO study group (2002) A phase II study of topotecan plus gemcitabine in the treatment of patients with relapsed ovarian cancer after failure of first-line chemotherapy. *Ann. Oncol. 13*, 1749–55.
(30) Allen, T. M., and Cullis, P. R. (2004) Drug delivery systems: entering the mainstream. *Science 303*, 1818–22.
(31) Wosikowski, K., Biedermann, E., and Rattel, B. (2003) In vitro and in vivo antitumor activity of methotrexate conjugated to human serum albumin in human cancer cells. *Clin. Cancer Res. 9*, 1917–26.
(32) Burger, A. M., Hartung, G., Stehle, G., Sinn, H., and Fiebig, H. H. (2001) Pre-clinical evaluation of a methotrexate-albumin conjugate (MTX-HSA) in human tumor xenografts in vivo. *Int. J. Cancer 92*, 718–24.
(33) Dennis, M. S., Zhang, M., Meng, Y. G., Kadkhodayan, M., Kirchhofer, D., Combs, D., and Damico, L. A. (2002) Albumin binding as a general strategy for improving the pharmacokinetics of proteins. *J. Biol. Chem. 38*, 35035–43.
(34) Felix, K. (2008) Albumin as a drug carrier: Design of prodrugs, drug conjugates and nanoparticles. *J. Controlled Release 132*, 171–83.
(35) Bickel, U., Yoshikawa, T., and Pardridge, W. M. (2001) Delivery of peptides and proteinsthrough the blood-brain barrier. *Adv. Drug Delivery Rev. 46*, 247–79.
(36) Lu, W., Sun, Q., Wan, J., She, Z., and Jiang, X. G. (2006) Cationic albumin-conjugated pegylated nanoparticles allow gene delivery into brain tumors via intravenous administration. *Cancer Res. 66*, 11878–87.
(37) Seki, T., Fang, J., and Maeda, H. (2009) Enhanced delivery of macromolecular antitumor drugs to tumors by nitroglycerin application. *Cancer Sci. 100*, 2426–30.

Characterization of the Hepatic Cellular Uptake of α_1-Acid Glycoprotein (AGP), Part 1: A Peptide Moiety of Human AGP Is Recognized by the Hemoglobin β-Chain on Mouse Liver Parenchymal Cells

KOJI NISHI,[1,2] HISAKAZU KOMORI,[1] MARI KIKUCHI,[1] NAO UEHARA,[1] NAOKO FUKUNAGA,[1] KAZUAKI MATSUMOTO,[1] HIROSHI WATANABE,[1,3] KEISUKE NAKAJOU,[1] SHOGO MISUMI,[4] AYAKA SUENAGA,[1] TORU MARUYAMA,[1,3] MASAKI OTAGIRI[1,5]

[1]Department of Biopharmaceutics, Graduate School of Pharmaceutical Sciences, Kumamoto University, Kumamoto, Japan

[2]Department of Clinical Pharmacokinetics and Pharmacodynamics, School of Medicine, Keio University, Tokyo, Japan

[3]Center for Clinical Pharmaceutical Sciences, School of Pharmacy, Kumamoto University, Kumamoto, Japan

[4]Department of Pharmaceutical Biochemistry, Graduate School of Pharmaceutical Sciences, Kumamoto University, Kumamoto, Japan

[5]Faculty of Pharmaceutical Sciences, Sojo University, Kumamoto, Japan

Received 29 July 2011; revised 2 September 2011; accepted 14 October 2011

Published online 11 November 2011 in Wiley Online Library (wileyonlinelibrary.com). DOI 10.1002/jps.22804

ABSTRACT: Human α_1-acid glycoprotein (AGP), a serum glycoprotein, is known to have anti-inflammatory activity. We recently reported that AGP was mainly incorporated into the liver in mice via a receptor-mediated pathway, although the mechanism for this was largely unknown. The objective of this study was to identify the specific cellular surface protein that recognizes the peptide moiety of AGP. Pharmacokinetic studies of ^{111}In–AGP and ^{111}In –recombinant glycan-deficient AGP (rAGP) in mice demonstrated that both AGPs are mainly distributed to the liver and kidney, but hepatic and renal uptake clearance of rAGP was higher than that for AGP. Hepatic uptake of rAGP was inhibited in the presence of 100-fold excess of unlabeled AGP, indicating that the hepatic uptake of rAGP shared a common route with that of AGP and that it recognized the peptide moiety of AGPs. In ligand blotting analyses using crude cellular membrane fraction of mice liver, a band corresponding to a 16 kDa protein was observed to bind to both AGPs. Interestingly, matrix-assisted laser desorption ionization–time-of-flight mass spectrometry MALDI–TOF-MS and western blotting analyses indicated that this 16 kDa protein is the hemoglobin β-chain (HBB). It, therefore, appears that HBB is associated with the hepatic uptake of AGP via a direct interaction with its peptide moiety. © 2011 Wiley Periodicals, Inc. and the American Pharmacists Association J Pharm Sci 101:1599–1606, 2012

Keywords: alpha 1-acid glycoprotein; glycoproteins/glycoprotein receptors; distribution; kinetics; hepatic transport; protein binding

INTRODUCTION

Human α_1-acid glycoprotein (AGP), a serum glycoprotein, is composed of 183 amino acid residues and also contains five glycan chains, which account for about 40% of its total mass of 40 kDa.[1–4] AGP is a member of the lipocalin family of proteins, which function as carriers for small hydrophobic compounds.[5,6] In fact, AGP is a major carrier protein for basic drugs in the blood and plays a role in regulating their tissue distribution.

α_1-Acid glycoprotein has been reported to have anti-inflammatory activities as biological functions *in vivo* and *in vitro*.[7–10] It has been reported that AGP inhibits the apoptosis of hepatocytes in mice and primary rat hepatocytes via suppressing the activation of caspase.[11–13] In renal cells, AGP is also known to

Correspondence to: Toru Maruyama (Telephone: +81-96-371-4150; Fax: +81-96-362-7690; E-mail: tomaru@gpo.kumamoto-u.ac.jp); Masaki Otagiri (Telephone: +81-96-371-4150; Fax: +81-96-362-7690; E-mail: otagirim@ph.sojo-u.ac.jp)

Koji Nishi and Hisakazu Komori contributed equally to this work.

Journal of Pharmaceutical Sciences, Vol. 101, 1599–1606 (2012)

have a protective effect against ischemia/reperfusion-induced apoptosis.[10] However, the mechanisms of these effects are currently unclear. Although these intracellular events are thought to be caused by external stimulation via some receptors, such receptors for AGP on liver or kidney cell surfaces have not been identified or characterized.

In studies using ^{111}In-labeled AGP, we recently reported that AGP is incorporated into the liver via a receptor-mediated pathway.[14] The asialoglycoprotein receptor (ASGPR), a well known C-type lectin, appears to be involved in the uptake of asialo-AGP by the liver.[15] Therefore, it is generally thought that AGP is recognized in some manner by ASGPR in the liver, but only after sialic acids have been removed from the end units of the attached glycans.[16] However, there appear to be no reports of the detection of asialo-AGP in human blood. In addition, our recent study showed that the uptake of AGP by the mouse liver did not compete with asialo-AGP and vice versa.[14] Ishibashi et al.[17] also reported that the pharmacokinetics of AGP in ASGPR knockout mice was comparable to that in normal mice.[17] These findings lead to the hypothesis that a specific uptake route, that recognizes the peptide moiety of AGP, is operative in hepatocytes. To date, receptors for AGP have been proposed in hepatocytes, the human adrenal cortex, the human intestinal epithelial cell line, HepG2 cells, rodent testis, and cultured microvascular endothelium,[18–21] but all appear to recognize the glycan portion of AGP such as the lectin-like receptor and ASGPR. In addition, there is no experimental evidence for the existence of proteins that recognize the peptide moiety of AGP in the liver.

The purpose of this study was to identify the specific cellular surface protein that recognizes the peptide moiety of AGP. To specify the role of the peptide moiety in hepatocellular uptake, we prepared a recombinant glycan-deficient AGP (rAGP) from a *Pichia* expression system by mutating the five Asn residues (to which glycan chains are attached) to Asp residues and studied the pharmacokinetics of AGP in mice using this protein. In addition, we explored the constitution of the AGP-binding protein in mice primary hepatocyte and human liver cell lines using ligand blotting, matrix-assisted laser desorption ionization–time-of-flight mass spectrometry (MALDI–TOF-MS), and western blotting. The findings indicate that the protein in question is the hemoglobin β-chain (HBB).

MATERIALS AND METHODS

Materials and Animals

α_1-Acid glycoprotein was purchased from Sigma–Aldrich Company (St. Louis, Missouri). ^{111}Indium was a gift from Nihon Mediphysics (Tokyo, Japan). All other chemicals were of reagent grade or of the highest purity available commercially. Male ddY mice (24–26 g) were purchased from Japan SLC (Shizuoka, Japan). The animals were maintained under conventional housing conditions. All animal experiments were carried out in accordance with the guideline principles and procedures of Kumamoto University for the care and use of laboratory animals.

Preparation of rAGP

Recombinant glycan-deficient AGP complementary DNA was constructed by creating mutations of all five Asn residues (15, 38, 54, 75, and 85) to Asp residues using appropriate primers. The expression and purification of rAGP was performed as previously described.[22] After purification, we confirmed that far-ultraviolet circular dichroism spectrum of rAGP was comparable to that of AGP (data not shown).

Pharmacokinetic Experiments

To compare the pharmacokinetic properties of AGP and rAGP, both proteins were labeled with ^{111}In, as described previously.[14] The labeled AGPs were injected via the tail vein of mice at a dose of 0.1 mg/kg. Radioactivity was determined using a well-type NaI scintillation counter. Hepatic uptake clearance was calculated from integration plots.[23,24]

Cellular Experiments with Mouse Liver

Parenchymal, endothelial, and Kupffer cells from mouse livers were isolated according to our previous reports.[14] Three hours before the experiments, the medium was replaced with Dulbecco's modified Eagle's medium containing 3% bovine serum albumin. Five hours after the incubation, the medium was removed and the cells were washed three times with PBS and then dissolved in 0.1 N NaOH. The radioactivities of the solubilized cells were counted to calculate the amount of AGPs that had accumulated in the cells.

Ligand Blotting Experiments

α_1-Acid glycoprotein and rAGP were radiolabeled with $Na^{125}I$ using IODO-GEN® Iodination Reagent (Thermo Fisher Scientific, Rockford, IL). An aliquot of 40 μL of phosphate buffer (pH 7.4) and 160 μL of 20 mg/mL of AGP solution were added to an IODO-GEN® coated tube. The solutions were mixed well and 10 μL of $Na^{125}I$ was then added to the mixture solution. After incubation for 30 min at room temperature, the radiolabeled AGPs were purified by gel filtration using a PD-10 column. The crude liver membrane fraction of the cells was subjected to SDS–PAGE and electroblotted onto PVDF membranes. After blocking in 2% skim milk, the PVDF membrane was incubated

with a ^{125}I–AGP solution for 2 h. After washing and drying the PVDF membrane, radioactivity was measured using a Bio Imaging Analyzer (Fujifilm Company, Ltd., Tokyo, Japan).

Western Blot Analysis

Electroblotted PVDF membranes were incubated in 5% skim milk. The membranes were washed three times and verified with a human hemoglobin polyclonal antibody (Bethyl laboratories, Inc., Montgomery, TX). After washing three times, the membrane was incubated with a horseradish peroxidase -conjugated secondary antibody. Bands were detected using the SuperSignal West Pico chemiluminescent substrate (Pierce Biotechnology Inc.) according to the manufacturer's description.

MALDI–TOF-MS Analysis

After two-dimensional (2D) SDS–PAGE of the liver membrane fraction, the bands corresponding to the targeted protein and a control were cut off from the gel. After incubation with trypsin and purification, the sample was analyzed by MALDI–TOF-MS. From the molecular weights of peptides, a search for the candidate protein was initiated using the peptide database, MS-Fit (ProteinProspector version 5.9.0, University of California, San Francisco, California).

Data Analyses

Data are shown as mean ± SD for the indicated number of animals. Overall differences between groups were determined by one-way analysis of variance. A probability value of $p < 0.05$ was considered to indicate statistical significance.

RESULTS

Pharmacokinetics of AGP and rAGP

Figure 1a shows the pharmacokinetics of ^{111}In–AGP, ^{111}In–rAGP, and ^{111}In–rAGP with a 100-fold excess of unlabeled AGP in mice. The plasma radioactivity after administration of ^{111}In–AGP or ^{111}In–rAGP decreased dramatically within 5 min. rAGP was more rapidly eliminated from blood than AGP. In addition, the elimination of rAGP was suppressed in the presence an excess of AGP. This result suggests that AGP and rAGP are incorporated into tissues via a common receptor and that the receptor recognizes a peptide moiety of AGP during the process of elimination.

Figure 1b shows the data on the tissue distribution of ^{111}In–AGP, ^{111}In–rAGP, and ^{111}In–rAGP in the presence of excess unlabeled AGP at 2 h after administration. AGP was mainly distributed to the liver, as previously reported,[14] whereas rAGP was distributed to both liver and kidney. In addition, radioactivity was recovered in urine after administration of ^{111}In–rAGP. It seems that rAGP excreted into urine by glomerular filtration because the molecular weight of rAGP was about 20 kDa, which is small enough to be excreted in urine. The distribution of rAGP to the liver was also suppressed to a significant extent in the presence of excess AGP. The distribution of rAGP to the kidney was suppressed slightly in the presence of excess AGP. Indeed, the uptake clearance values for AGP and rAGP reflect the results for tissue distribution (Fig. 1c).

Hepatocellular Distribution of AGP and rAGP

Because we previously found that AGP was mainly distributed to parenchymal cells in mice hepatocytes, these experiments were repeated for rAGP (Table 1). Similar to AGP, the majority of rAGP was incorporated into parenchymal cells. This result suggests that rAGP interacts with a protein that is localized in parenchymal cells, the same as AGP. It was observed that the uptakes of rAGP to Kupffer and endothelial cells were increased slightly as compared with the corresponding values for AGP.

Ligand Blotting Analysis of Liver Membrane Fraction with ^{125}I–AGP and ^{125}I–rAGP

To identify the protein that interacts with AGP and rAGP on the hepatocellular surface, we performed a ligand blotting analysis of ^{125}I–AGP and ^{125}I–rAGP with the crude membrane fraction of mice hepatocytes (Fig. 2). In this experiment, proteins that interact with ^{125}I–AGP and ^{125}I–rAGP appear as radioactive bands on the PVDF membrane. A large number of bands on lane 2 were stained with coomassie brilliant blue (CBB). Among them, several bands, corresponding to 30, 27, and 16 kDa proteins, were strongly radioactive. Interestingly, it was observed that rAGP interacted with the 16 kDa protein (lane 3), which appeared to be identical to the band observed in lane 2. This suggests that AGP binds to this 16 kDa protein via peptide–peptide interactions. In the same experiment using rat liver primary parenchymal cells, we also found that AGP interacted with this 16 kDa protein (data not shown). Considering the results shown in Table 1, it can be assumed that the 16 kDa protein is present on the membrane surface of liver parenchymal cells.

Identification of the AGP-Binding Protein on Hepatocytes

After separation and purification of the 16 kDa protein from the membrane fraction of mice livers by 2D PAGE (Fig. 3a), a MALDI–TOF-MS analysis was carried out on the product. Table 2 shows the molecular weights of peptides that were obtained by trypsin digestion, as obtained from a MALDI–TOF-MS analysis. On the basis of the molecular weights of these

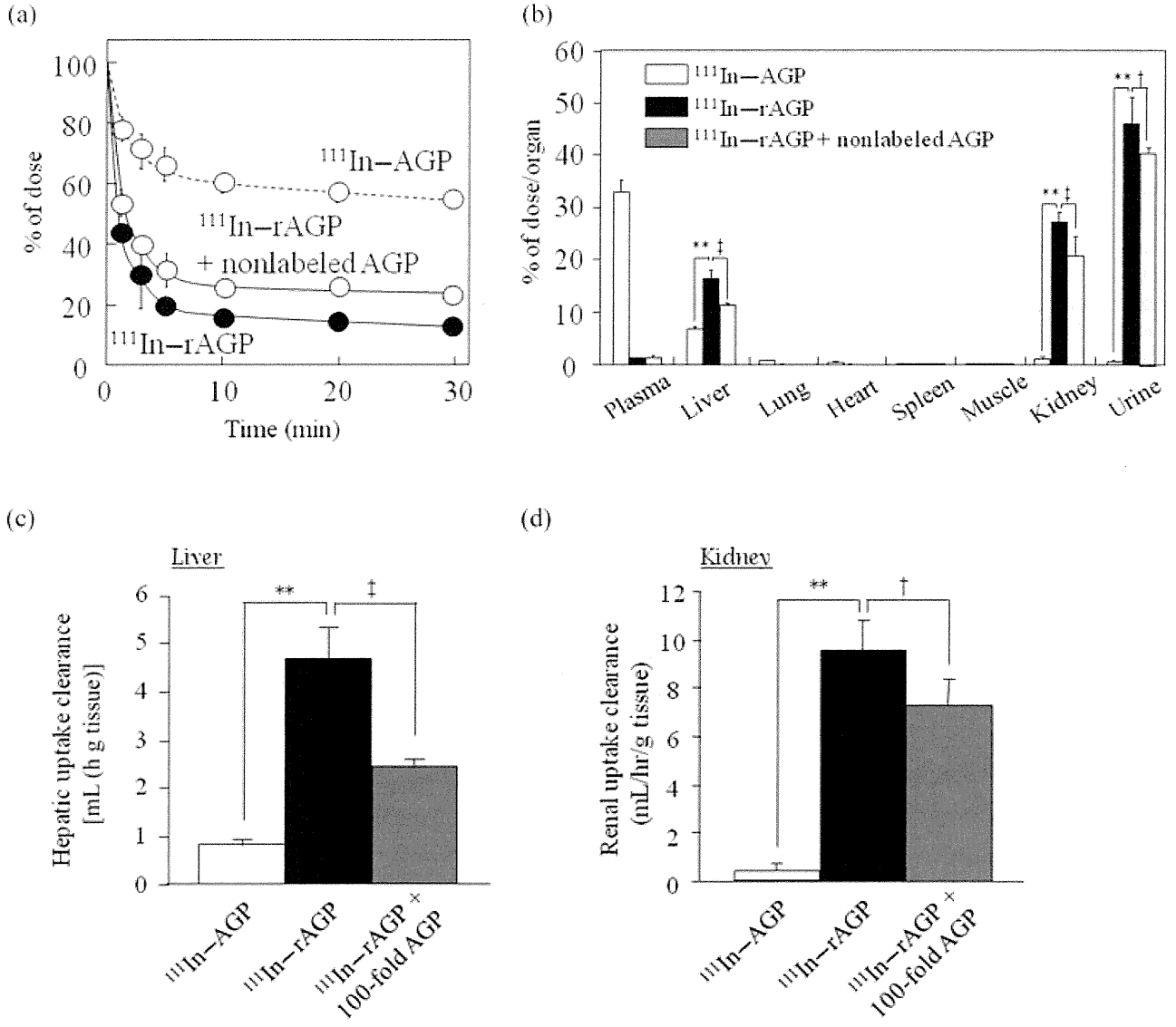

Figure 1. Pharmacokinetics of ^{111}In–AGP, ^{111}In–rAGP, and ^{111}In–rAGP in the presence of excess AGP in mice. (a) Time-dependent elimination of ^{111}In–AGP and ^{111}In–rAGP from blood. (b) Tissue distributions of ^{111}In–AGP and ^{111}In–rAGP 2 h after administration. (c) Uptake clearance values of ^{111}In–AGP and ^{111}In–rAGP in liver and kidney. Each data point represents the mean ± SD of three independent experiments. $**p < 0.01$, statistically significant increase compared with ^{111}In–AGP; $\dagger p < 0.05$ and $\ddagger p < 0.01$, statistically significant decrease compared with ^{111}In–rAGP.

peptides, the candidate 16 kDa protein was explored using the peptide database, MS-Fit. After screening this database, the 16 kDa protein was determined to be the HBB.

To confirm the results of the MS analysis, we performed 2D ligand blotting with ^{125}I–AGP and western blotting analyses of primary parenchymal cells from mice livers (Fig. 3). Many bands were observed in the CBB staining of primary parenchymal cells from mice livers (Fig. 3a), whereas the band with radioactivity appeared at around p*I* 7.5 (Fig. 3b). Furthermore, the only band with an anti-hemoglobin polyclonal antibody appeared at the same position (Fig. 3c). From the 2D PAGE database, the p*I* value for HBB and the hemoglobin α-chain was found to be around 7.5 and 9.0, respectively.[25,26]

The same experiments were conducted using a HepG2 cell line. As shown in Figure 4, the pattern for the bands of primary parenchymal cells from mice livers stained with CBB was quite different from the pattern obtained for the HepG2 cells, whereas the band was similarly obtained at around 16 kDa. Again, these radioactive bands reacted with an anti-hemoglobin polyclonal antibody (Figs. 4b and 4c). Collectively, these data suggest that the band observed for primary hepatocytes (Fig. 3c) is HBB, which excludes the possibility that the HBB detected in hepatocytes was derived from a blood-derived contaminant.